BIFUNCTIONAL CATALYSTS WITH IMPROVED HYDROTHERMAL STABILITY FOR THE HYDROLYTIC HYDROGENATION OF CELLULOSE INTO POLYOLS

by

Darlene Zoe Galloza Lorenzo

A dissertation submitted in partial fulfillment of the requirements for the degree of

DOCTOR OF PHILOSOPHY

in

CHEMICAL ENGINEERING

UNIVERSITY OF PUERTO RICO

MAYAGÜEZ CAMPUS

2014

Approved by:

_____   _____
Nelson Cardona, PhD   Date
President, Graduate Committee

_____   _____
María Curet, PhD   Date
Member, Graduate Committee

_____   _____
María Martínez, PhD   Date
Member, Graduate Committee

_____   _____
Arturo Hernández, PhD   Date
Member, Graduate Committee

_____   _____
José Cortés, PhD   Date
Representative of Graduate Studies

_____   _____
Aldo Acevedo, PhD   Date
Chairperson of the Department

Bifunctional Catalysts with Improved Hydrothermal Stability for the Hydrolytic Hydrogenation of Cellulose into Polyols

by Darlene Z. Galloza Lorenzo

Submitted to the Graduate School of the University of Puerto Rico
in Partial Fulfillment of the Requirements for the Degree of Doctor of Philosophy
2014

ABSTRACT

The increase in the world's energy needs has caused a renewed interest in finding green ways to produce fuels. In this work, we present a study of the hydrolytic hydrogenation of cellulose on bifunctional catalysts for the production of glucose and/or sorbitol. These molecules offer the potential to be used as renewable feedstock in a biorefinery for the production of fuels and value added chemicals. We report results for the study of the effects of: cellulose crystallinity, cellulose/catalyst ratio, the acid functionality, the hydrothermal stability, reaction temperature and reaction time on the catalytic performance for the conversion of cellulose into sorbitol. A series of single, binary and ternary metal oxide supports with a range of surface acidity, transition metal (V) phosphate and zeolites, were studied. Ruthenium was supported using evaporative deposition on the supports.

Our results show that the hydrolysis catalytic activity for the single metal oxide supports correlate with the Sanderson electronegativity of the metal oxide, passing through a maximum for Nb_2O_5 (HY 340). The Lewis acidity of the metal oxide also correlates well with the Sanderson electronegativity of the sample. However, when ruthenium is supported on the metal oxides they all displayed comparable catalytic performance that was similar to the performance observed in a reaction without catalyst. This result suggests that the change in product distribution causes a leveling effect on the hydrolysis activity. The absence of carboxylic

acids when the bifunctional catalysts are used explains the decrease in apparent catalytic activity. Under these reaction conditions the rate determining step, i.e., the initial hydrolysis of cellulose is not promoted by the bifunctional catalyst but rather by the hydronium ions present in water at the reaction conditions. The addition of Brønsted acidity by phosphating niobium or tantalum oxide significantly enhances the hydrolysis of cellulose. Of all catalytic materials tested, ruthenium supported on $NbOPO_4$ displayed the best catalytic performance with hexitols yields of about 45% at 100% cellulose conversion. All materials suffer changes in their properties after treatment in hot water. However, treating the catalysts based on transition metal (V) phosphate in water at 503 K and 35 bar H_2 for 24 h or 48 h caused a slight decrease in cellulose conversion, but a significant increase in hexitol and hydrogenolysis products yield. Ru/Nb_2O_5 (HY 340) and the equivalent amount of phosphoric acid present in $Ru/NbOPO_4$, give essentially the same conversion as $Ru/NbOPO_4$, but a lower yield to sugar alcohols and a higher yield to hydrogenolysis products. Decreasing cellulose crystallinity and cellulose/catalyst ratio, increases the cellulose conversion and hexitols yield for $Ru/NbOPO_4$.

Catalizadores Bifuncionales con Mejor Estabilidad Hidrotérmica para la Hidrogenación Hidrolítica de Celulosa a Polioles

por Darlene Z. Galloza Lorenzo

RESUMEN

El aumento de las necesidades energéticas del mundo ha provocado un interés de encontrar vías verdes para producir combustibles. En este trabajo presentamos un estudio de la hidrogenación hidrolítica de celulosa sobre catalizadores bifuncionales para la producción de glucosa y/o sorbitol. Estas moléculas ofrecen el potencial de ser utilizadas como materia prima renovable en una biorefinería para la producción de combustibles y productos químicos de valor añadido. Presentamos resultados para el estudio de los efectos de: la cristalinidad de celulosa, la relación de celulosa/catalizador, la funcionalidad acídica, la estabilidad hidrotérmica, temperaturas de reacción y tiempos de reacción sobre el rendimiento catalítico para la conversión de la celulosa a sorbitol. Una serie de soportes de óxidos metálicos simples, binarios y ternarios con un rango de acidez de la superficie, metales de transición (V) de fosfato y zeolitas, se estudiaron. Rutenio fue depositado usando deposición por evaporación sobre los soportes.

Nuestros resultados muestran que la actividad catalítica para la hidrólisis de los soportes simples de óxido de metal se correlaciona con la electronegatividad de Sanderson, pasando a través de un máximo para Nb_2O_5 (HY 340). La acidez Lewis de los óxidos metálicos también correlaciona bien con la electronegatividad Sanderson de la muestra. Sin embargo, cuando rutenio se deposita sobre los óxidos metálicos, todos muestran un comportamiento catalítico que es similar al desempeño observado en una reacción sin catalizador. Este resultado sugiere que el

cambio en la distribución de productos causa un efecto que nivela la actividad para hidrólisis. La ausencia de ácidos carboxílicos cuando se utilizan catalizadores bifuncionales explica la disminución en actividad catalítica. Bajo esas condiciones de reacción el paso de tasa determinante, i.e. la hidrólisis inicial de celulosa no es promovida por los catalizadores bifuncionales sino por los iones hidronio presentes en agua a las condiciones de reacción. De todos los materiales catalíticos puestos a prueba, rutenio sobre $NbOPO_4$ muestra el mejor rendimiento catalítico con un rendimiento para hexitoles de aproximadamente 45% para una conversión de 100% celulosa. Todos los materiales sufrieron cambios en sus propiedades después de los tratamientos con agua caliente. Sin embargo, el tratamiento de los catalizadores basado en los metales de transición (V) de fosfato en agua a 503 K y 35 bar de H_2 durante 24 h o 48 h causó una ligera disminución en la conversión de celulosa, pero un aumento significativo en los rendimientos para hexitoles y productos de hidrogenólisis. Ru/Nb_2O_5 (HY 340) y la cantidad equivalente de ácido fosfórico presente en $Ru/NbOPO_4$, da esencialmente la misma conversión como para $Ru/NbOPO_4$ pero con rendimientos bajos para los alcoholes de azúcar y un mayor rendimiento para los productos de hidrogenólisis. La disminución de la cristalinidad de celulosa y la relación de celulosa/catalizador, aumenta la conversión de celulosa y el rendimiento de hexitoles para $Ru/NbOPO_4$.

To my parents, Daniel and Carmen.

My sister, Marlene and my husband Isaac.

ACKNOWLEDGEMENTS

I want to express a sincere gratitude to my advisor, Dr. Nelson Cardona Martínez, for all the confidence, knowledge, teaching and the opportunity to perform research under his guidance and supervision. Additionally, to my thesis committee: Dr. María Curet Arana, Dr. María Martínez Iñesta and Dr. Arturo Hernández Maldonado, for all the discussions, and feedback to finish this dissertation. Further, I am very grateful to Dr. María Martínez-Iñesta, Dr. Arturo Hernández-Maldonado and their graduate students for allowing the use of their instrumentation.

Also, I want to thank my lab partners from NCML, for the help, the training, and for all the scientific discussions, that taught me to be a better scientist. To Audrey Michelli for the synthesis of the mesoporous carbon material (CMK-3) and Marietta Marcano for the synthesis of UPRM-5 titanium silicate. Moreover, thanks to Dr. Carlos Velázquez and Dr. David Mota for the analysis of particle size distribution. In the same way, I want to thanks Dr. Rafael Méndez for the synthesis and the pyridine adsorption analysis of the binary metal oxides materials. Additionally, to Dr. James Dumesic and Dr. Ana Alba Rubio at the University of Wisconsin-Madison for the STEM analysis. Furthermore, I appreciate the Chemical Engineering Department at the University of Puerto Rico at Mayagüez, for giving me the opportunity to continue my graduate studies.

Most importantly, I want to give my sincere thanks to all my family for their motivation, support and blessings during my studies. To my friends for your help, support and encouragement. Also, I am deeply grateful to my parents and my sister, for always been my support and my sustain in all my decisions. In the same way, I am more than grateful to my husband, Isaac Torres, for the motivation, the lessons and for being my example to never give up and follow my dreams.

TABLE OF CONTENTS

TABLE LIST

FIGURE LIST

1 **INTRODUCTION**

1.1 Motivation

The increase of the world's energy needs with the combination of several factors including the diminishing of petroleum resources, the increase in the petrochemicals prices, as well as the increase of green house gases emissions, has caused great interest in finding new processes to produce renewable fuels. Statistical reviews of the world's energy reveal that the world oil reserves in 2012 were sufficient to last 52.9 years, while North America only had reserves for 38.7 years.[1] The combustion of fossil fuels to produce energy for transportation and electricity, helped humanity achieve a simpler daily life, but also caused an increase in the concentration of greenhouse gas emissions since the Industrial Revolution.[2]

The CO_2 emissions total count are based on the concentrations obtained from the ocean and land reservoirs.[3] The expected CO_2 atmospheric concentration by 2040 for the developed countries will decrease by 20% when compared to the values in 2010, as long as mankind uses energy efficient technologies and less carbon-intensive fuels.[4] On the other hand, the increase in population, the creation of new technologies, the change in the economy, among many others, is expected to cause a chain reaction of fuel demand and increase in CO_2 concentration.[2] The increase in greenhouse gas emissions will also create changes in the Earth atmosphere, which eventually produces climate changes such as an increase in ocean temperatures, levels and acidity; changes in snow and rain fall patterns and their intensity; changes in cyclone activity, the durability of drought due to an increase in temperature, and also influence the melting of sea ice and glaciers.[2]

As a result an increase in the use of renewable energy sources such as hydroelectric, solar, geothermal, wind power and biomass are required to supply the demand for energy. Furthermore, the annual global energy consumption is in the same order of magnitude as the amount of biomass that could be produced worldwide for these purposes.[5] Biomass is the main natural resource that can give the basic elements that are essential in the production of fuels and chemicals, such as carbon and hydrogen that are produced in abundant amounts from the photosynthesis reaction.[6,7] The use of biomass as energy source, either converting carbohydrates to specific classes of hydrocarbons for the use as liquids fuels, like branched hydrocarbons and aromatic compounds for the production of gasoline, or longer chain, less highly branched hydrocarbons for producing diesel and jet fuels.[8] For the production of liquid transportation fuels requires the transformation of the feedstock into molecules with desirable properties for combustion with the removal of most of the oxygen atoms.[8]

1.2 Biomass

The plant components that are included in the non edible lignocellulosic biomass are cellulose, hemicellulose and lignin, these three are the components of the cell wall of plants as seen in Figure 1-1.[6,7,9] The composition of biomass depends on its origin. Mostly biomass is composed of 20-30 % lignin, 20-40 % of hemicellulose and finally 40-50 % of cellulose.[10,11] Additionally, biomass contains a much richer oxygen content, than petroleum derivatives, such as coal, crude oil and gas.[12]

Hemicellulose is a polymer composed of various monosaccharides of 5 and 6 carbons, like arabinose, glucose, galactose, mannose and xylose, linked together in various forms and is easy to hydrolyze.[7,13] On the other hand, the composition of the polymer lignin is of aromatic

lignols composed of p-coumaryl, coniferyl and sinapyl alcohols that lack a defined structure. Lignin gives strength to the woods of trees and protection to the cell walls.[13] Cellulose is also a polymer composed of D-glucose monomers connected with ß-1, 4-glycosidic bonds. It is not soluble in water and it is not digestible by humans.[6,7,9,14–17] Cellulose typically has both amorphous and crystalline structures. Cellulose has hydroxyl groups and hydrogen bonds that give rise to strong crystalline structure domains, due to the high tensile strength of the microfibrils of the cell wall.[11,18] Instead, the amorphous domains in the microcrystalline cellulose, possess a completely different structure, length and strength, that allows easy access to small molecules like for example water that can penetrate in this region.[18] Cellulose uses can be found in lumber, fuel, textile, paper, plastics, etc.[9,14] Additionally, it holds significant potential as an alternative renewable feedstock for the sustainable production of fuels and chemicals. With 35-50% of the annual net yield of photosynthesis, cellulose is the most abundant natural source from biomass.[9,14,15,19,20]
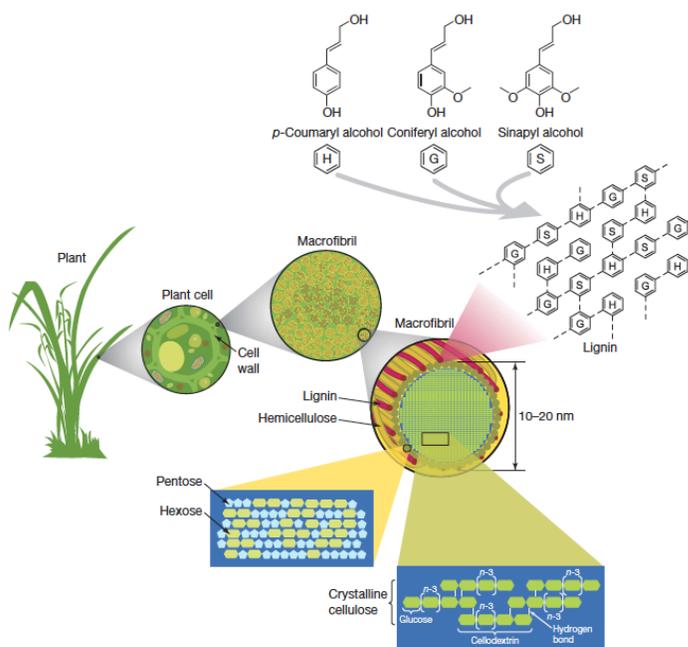
Figure 1-1. Structure of lignocellulosic biomass.[21]

Cellulose　　　　**Glucose**　　　　**Sorbitol**
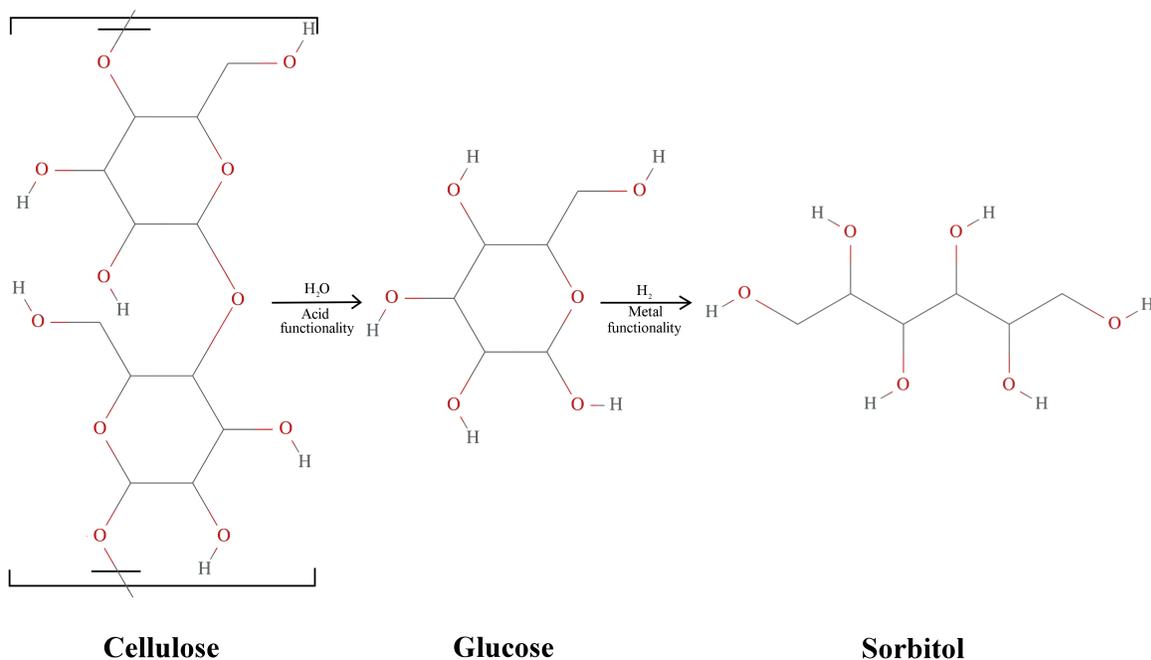
Figure 1-2. Catalytic conversion of cellulose into sorbitol.

Cellulose can be converted by hydrolysis with the aid of an acid or base functionality of the support into sugars like glucose and then with the metal functionality of the catalyst it may be hydrogenated to obtain sorbitol and other polyols (Figure 1-2) that can be used in a biorefinery platform to produce liquid transportation fuels as seen in Figure 1-3.[5,15] Therefore, the production of fuels from biomass is a way of helping meet the fuel demand, as well as reducing the emission of CO_2 that should help control climate change that is affecting our planet.
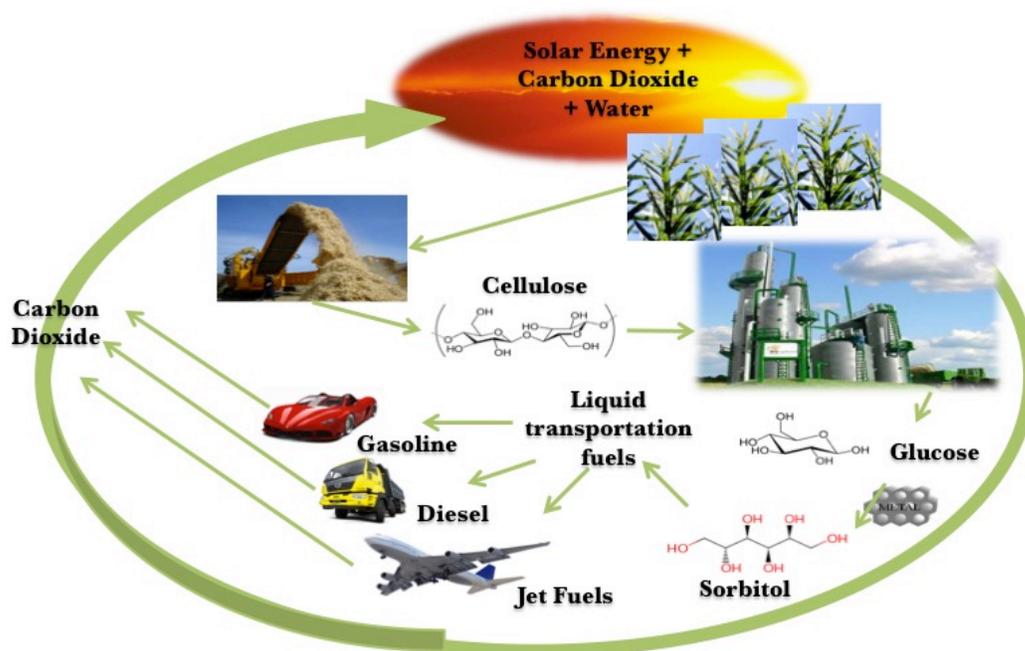
Figure 1-3. Biorefinery cycle.

Cellulose can be converted into valuable products such as glucose and/or sorbitol, as mentioned before. Based on these two products, polymers, chemicals and fuels can be obtained. Gluconic acid can be produced from the oxidation of glucose, which is mainly used in pharmaceutical, food and biological industries.[22] Fructose can be obtained from the isomerization of glucose, which in turn may be dehydrated to produce 5-hydroxymethylfurural (HMF).[23,24] HMF is a platform molecule for many chemicals, polymers and fuels production, like formic acid, levulinic acid, 2, 5-furandicarboxylic acid, among others.[25] Compounds like glycerol, erythritol and ethylene glycol can be obtained by sorbitol hydrogenolysis.[23] Sorbitan and isoborbide are formed from the dehydration of sorbitol, which are used as surfactants and monomers.[26] Additionally, glucose and/or sorbitol can be used as a biorefinery feedstock,[5,15] for the production of liquid transportations fuels from catalytic processes.[8] Dumesic and coworkers developed a process to produce liquid transportation fuels involving a combination of processes

like catalytic reforming, de-oxygenation, dehydration, isomerization, alkylation, aromatization, C-C coupling, hydrogenation and hydrodeoxygenation as seen in Figure 1-4.[8]
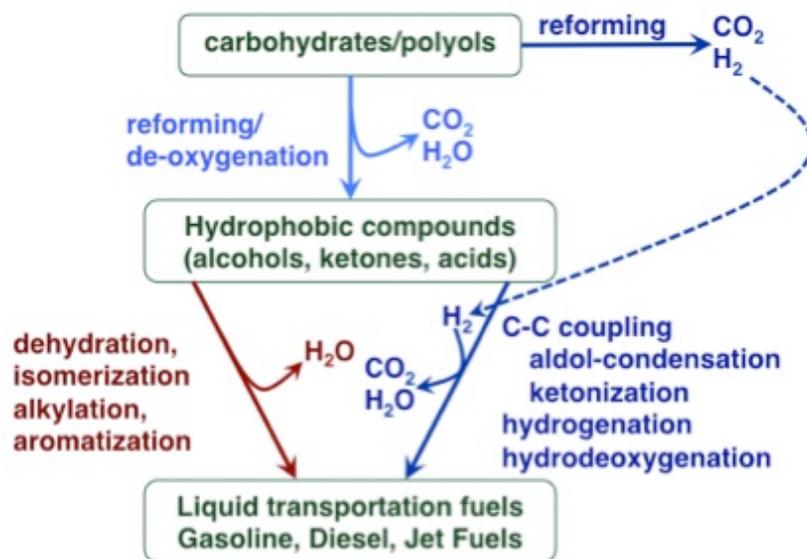
Figure 1-4. Strategies for converting carbohydrates and polyols in liquid transportation fuels.[8]

1.3 Catalyst

Catalysis is the study of materials that increase the rate at which products are formed, during a chemical reaction, providing an alternative route.[27–29] The alternate path is more energy favorable providing a lower effective activation energy for the reaction as seen in Figure 1-5.[27,29] During reaction there will be a series of steps in which these materials called catalysts are involved, first the reactants molecules form a bond with the catalysts allowing them to react to form the products, finally the products will separate from the catalyst to be used in another cycle.[29]
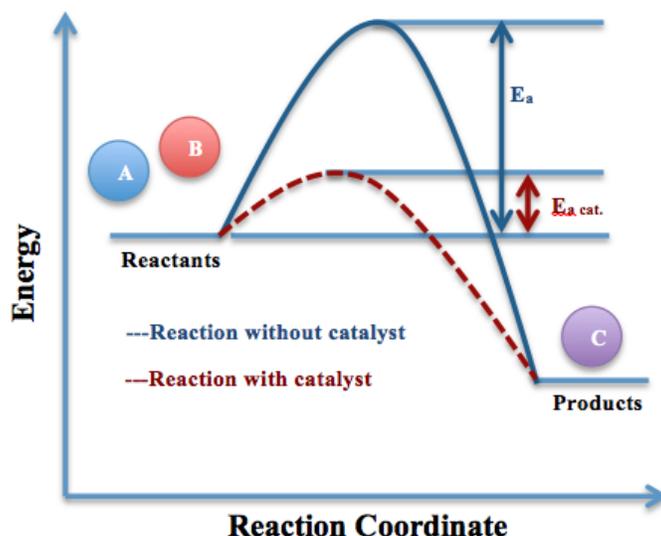
Figure 1-5. Comparison of the energy of a stoichiometric reaction with that for a catalytic reaction as a function of the reaction coordinate.

Catalysts can be acids, metals, enzymes and so on, for this they are classified as biocatalysts, homogenous and heterogeneous catalysts.[27–29] Biocatalysts are enzymes that catalyze organic reactions.[28] Pepsin and catalase are some examples of catalysts that are enzymes that help in the digestion of food proteins or decomposing hydrogen peroxide in the human body.[29–34] The catalysts that are in the same physical state as one of the reactants are called homogenous catalysts.[27–29] Furthermore, heterogeneous catalysts are materials that are in a different phase than the reactants or products.[27–29] Usually, there are solid materials, like for example noble metals as platinum, rhodium and palladium typically deposited on the monoliths of the catalytic converters for cars.[29,35–37] Other examples are metal oxides and zeolites that are highly used as catalysts in the petrochemical industry.[29]

1.4 Catalytic conversion of cellulose

1.4.1 Hydrolysis reaction

The hydrolysis of cellulose or carbohydrates has been tested with the use of ionic liquids like 1-butyl-3-methylimidazolium chloride (BMImCl),[19,38] 1-alkyl-3-methylimidazolium chloride,[39] 1-allyl-3-methylimidazolium chloride (AMImCl),[19] 1-butyl-3-methylimidazolium dicyanamide,[40,41] among others.[19,38–43] Also, metal chlorides or mineral acids, like sulfuric acid and hydrochloric acid have been investigated for the hydrolysis of carbohydrates.[7,17,44–47] However, liquid acids are corrosive, need acid recovery and disposal, which makes those process not environmentally friendly. Additionally, certain enzymes such as cellulase have been used to hydrolyze cellulose, but low reaction rates, high processes costs, enzymes separation difficulties from the reaction media, makes this method expensive.[7,9,17,45,48–50] Supercritical water also has been used for the hydrolysis of cellulose. However, the major disadvantage of this method is the low glucose selectivity due to high temperature instabilities. Additionally, It may corrode the equipment and consumes much energy during operation.[7,9,17,45,51]

Solid catalysts with acidic properties have also been studied for the hydrolysis of cellulose. Layered transition metal oxide ($HNbMoO_6$) possess a strong acidic gallery, which contributed to obtain high activities for the hydrolysis of cellulose, cellobiose, starch and sucrose.[52] γ-Al_2O_3, SiO_2 and H-zeolites like Modernite, BETA and ZSM-5 were used for the hydrolysis of cellulose, and a dependency between the acidity and hydrolysis activity, was observed.[14] On the other hand, phosphated niobia was also investigated for the dehydration of fructose, the addition of the phosphate enhanced the acidity of the catalyst obtaining higher activities than niobium oxide, due to the strength of acid sites on the $NbOPO_4$.[53] The same acidic

behavior was also observed in other studies for the dehydration of glucose and fructose to 5-hydroxymethylfurfural using niobium and tantalum phosphate.[54–57]

Furthermore, other catalysts studied with the incorporation of a liquid acid or a functional group for the hydrolysis of cellulose have been sulfonated active carbon (AC-SO$_3$H),[14] sulfonic group functionalized magnetic mesoporous silica (Fe$_3$O$_4$-SBA-SO$_3$H),[58] sulfonated mesoporous carbon (CMK-3),[59] heteropoly acids (H$_3$PW$_{12}$O$_{40}$, Cs$_1$H$_2$PW$_{12}$O$_{40}$)[60,61] and sulfonated silica-carbon nanocomposites.[62] Additionally, amorphous carbon bearing SO$_3$H, COOH and OH groups were studied for this reaction, and high activities were obtained thanks to the ability of these materials to adsorb β-1, 4 glucan.[16] H-form zeolites like CBV-400, HY, HBETA, HZMS-5 were used with ionic liquids as solvents for the hydrolysis of cellulose to 5-hydroxymethylfurfural and presented an increase in catalytic performance of the zeolites studied, due to an increase in acidity by the use of the ionic liquids.[63,64] Furthermore, an increase in the amount of acidic sites on the zeolites itself, like when H-MOR catalyzed the reaction instead of H-BEA, an increase in HMF selectivity was observed.[65]

When, the hydrolysis of cellulose is performed using only the support (the acid functionality of the catalyst) many reactions occur at the same time. As mentioned before, cellulose is hydrolyzed and produces cellobiose and glucose. Additionally, sugars like arabinose and xylose also are obtained from the hydrolysis of hemicellulose, because the cellulose may have traces of hemicellulose. Isomerization of glucose is also observed, producing fructose and mannose. From the dehydration of fructose, arabinose, xylose and glucose, 5-hydroxymethylfurural (HMF), furfural and levoglucose products are obtained. Additionally, insoluble humins are formed by the polymerization of glucose and 5-hydroxymethylfurural in

acidic media.[54,55,66] The rehydration of 5-hydroxymethylfurural, yields acids like formic and levulinic acid. These reaction pathways are seen in Figure 1-6.
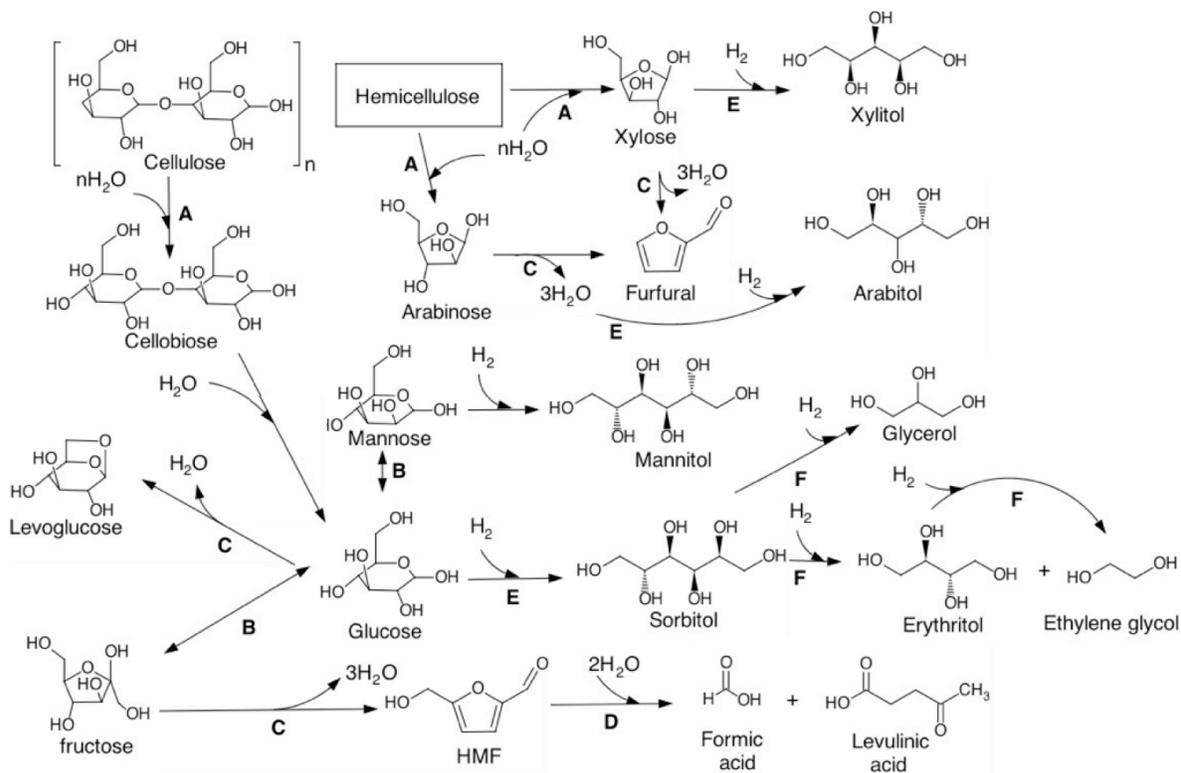
Figure 1-6. Reaction pathways for the conversion of cellulose to polyols. Hydrolysis (A), Isomerization (B), Dehydration (C), Rehydration (D), Hydrogenation (E), Hydrogenolysis (F).[23]

1.4.2 Carbohydrates hydrogenation

The incorporation of a metal functionality on solid catalysts is essential for the hydrogenation of cellulose.[10,12,13,18–20,67,68] The aim of the metal functionality is to hydrogenate the sugars like glucose, mannose, arabinose and xylose, to produce sugar alcohols like sorbitol, mannitol, arabitol and xylitol important for the production of fuels, as seen in Figure 1-6. The metal functionality also promotes the hydrogenolysis of hexitols from which we may obtain glycerol, erythritol and ethylene glycol. Additionally, the metal loading on the catalyst inhibits

dehydration and rehydration reactions that occur when only the support is present. Transition metals have been used for the hydrolytic hydrogenation of cellulose, because they have good activities for the hydrogenation of glucose. The first steps during the hydrolytic hydrogenation of cellulose involve the hydrolysis to produce poly and monosacharides. For this reason if the catalyst has an adequate surface acidity, it may increase the hydronium ion concentration in solution, helping improve the conversion of cellulose. Fukuoka *et al*. used chlorine precursors for Pt, Ru, Pd, Ir or Ni supported on a series of metal oxides that included γ-Al_2O_3, SiO_2-Al_2O_3 and zeolites. Some of these catalysts displayed high yields for sugar alcohols. They proposed that the metal functionality and the acidity was generated by hydrogen spillover.[9] The same proposition was suggested by Jollet *et al*. who used Pt/γ-Al_2O_3 for the dissolution of cellulose.[69] Furthermore, in a study with Ru/$NbOPO_4$ at different initial pHs and $RuCl_3$ as ruthenium precursor, the authors demonstrated that the high catalytic performance of this catalyst was partly due to the high acid amount of the catalyst.[70] However, Sievers *et al*. demonstrated that employing chlorine-containing metal precursors, causes an intense leaching of the support and a decrease in the point of zero charge, affecting eventually the catalytic performance, due to residual chlorine anions in solution that increase the conversion of cellulose.[71] Additionally, it was demonstrated, that with the use of chlorine precursors, the hydrolysis activity increases and the formation of by-products, due to the formation of HCl. On the other hand, the yield of sugar alcohols improved, when chlorine free metal precursors were used instead.[6]

As mentioned above transition metals supported on metal oxides have been studied for the hydrolytic hydrogenation of cellulose. It has been demonstrated, that the yield of polyols is affected by the loading and the transition metal used, in the hydrogenation of cellulose over nickel-promoted W-SiO_2-Al_2O_3 catalysts and Ni/γ-Al_2O_3.[72,73] Additionally, the atomic ratio of

11

the metals Sn/Pt in Pt-SnO$_x$/Al$_2$O$_3$, affects the hexitols yields.[74] Another study showed that the hydrogenation was influenced by the dispersion, crystal size and surface area of the metal, during the hydrogenation of cellobiose and glucose over Ni/ZSM-5.[75] Furthermore, in a work with Ru, Ir, Pd and Rh over BEA zeolite for the hydrolytic hydrogenation of cellulose, the authors concluded that the selectivities were influenced by the d-band width of these metals and the hydrogen pressures used for the reaction. They also indicated that ruthenium forms Brønsted acids in water as protons and [Ru(H$_2$O)$_5$OH]$^{2+}$, leading to high activities.[76] Another study showed that ruthenium gave the highest sorbitol yields, from a variety of transition metals studied, over CNT, SiO$_2$, Al$_2$O$_3$ and MgO.[67]

The addition of a mineral acid and the effect of the support were also investigated. For the combination of a heteropoly acid with Ru/C, the authors claimed that having higher H$_3$O$^+$ concentrations and longer reaction times were the key to obtain an increase in conversion of cellulose to sugar alcohols for H$_4$[Si(W$_3$O$_{10}$)$_4$] and H$_3$[P(W$_3$O$_{10}$)$_4$].[77] Instead, a similar combination of Ru/C but with hydrotreated cesium salts of heteropoly acids, displayed higher activities per proton than their fully protonated counterparts, due to their high surface acidity and hydrophobicity.[78] Moreover, a study of ruthenium supported on zeolites with added mineral acids, shows the importance of acid to metal ratio optimization, reflected in a fast hydrolysis and a high hydrogenation products activities.[79] Additionally, other bi-functional catalysts studied for the production of polyols with the addition of an acid such as ruthenium on sulfonated activated carbon (10%Ru/AC-SO$_3$H),[80] platinum, palladium and ruthenium on carbon with the addition of mineral acids.[81] Ru/SBA-15 functionalized with arenesulfonic acid was studied for the catalytic conversion of cellulose.[23] It was observed that the acid promotes the activity and that the metal functionality controls the selectivity towards sugar alcohols.[23] The disadvantage of many

12

functionalized supports is the leaching of their functional group, due to the instability in hot water, that causes the collapse and/or changes in the crystalline structure, loss of surface area and an apparent increase in activity during reaction.[23,82–84] The stability of metal oxides has been enhanced by adding coatings of carbon or a second metal oxide, on the surface of these metal oxides.[66,83,85]

1.5 Sorbitol

Sorbitol can be obtained from nature in fruits and seaweed, but in small proportions.[86] The U.S. Department of Energy ranks sorbitol as the number two compound in the list of building blocks with high value potential for the production of value added chemicals and materials (Figure 1-7).[87,88] The production per year of sorbitol reaches more than 1.2 million of tons.[89] Sorbitol, also referred as glucitol has been studied to be used as a biorefinery platform molecule for the production of liquid transportation fuels.[8] Additionally, it has been used for the production of chemicals, pharmaceuticals, personal products, food, textiles, polymers and for the synthesis of L-ascorbic acid (vitamin C).[76,88–91]

The derivative chemicals obtained from the hydrogenolysis of sorbitol are ethanol, glycerol, ethylene glycol and propylene glycol.[92] Ethanol is used as an additive to fuel or as a fuel; instead glycerol is used as an additive for foods, cosmetics and medicines.[92–96] Ethylene glycol and propylene glycol are employed in the production of polyesters resins, perfumes, inks, medicines, surfactants and functional fluids.[94,95] Sorbitan and isosorbide, also are obtained from sorbitol, but from a dehydration reaction.[97–101] Sorbitan is an intermediate molecule for the production of isosorbide, for which a double dehydration has to occur to obtain sorbitan.[101]

These two products are useful for the synthesis of polymers, such as polyethylene terephthalate, as surfactants, and in the manufacture of cosmetics, medicines and food aditives.[97–101]

On the other hand, lactic acid is also obtained from the conversion of sorbitol, via an alkaline hydrothermal conversion.[102] Lactic acid is mainly used in the food industry as a preservative, to improve flavor and as an additive. Additionally, it is employed in the pharmaceutical and cosmetic industry, and for the manufacture of leather, textiles and polymers like polylactic acid.[101,103,104] Hexane may also be produced from sorbitol, obtained from an aqueous phase dehydration/hydrogenation sequential reactions, and is mainly used as a fuel.[96,105,106] On the other hand, L-sorbose is produced from the oxidation of sorbitol.[107–109] This molecule is used in the production of vitamin C, which is used in food and the manufacture of medicines.[110]
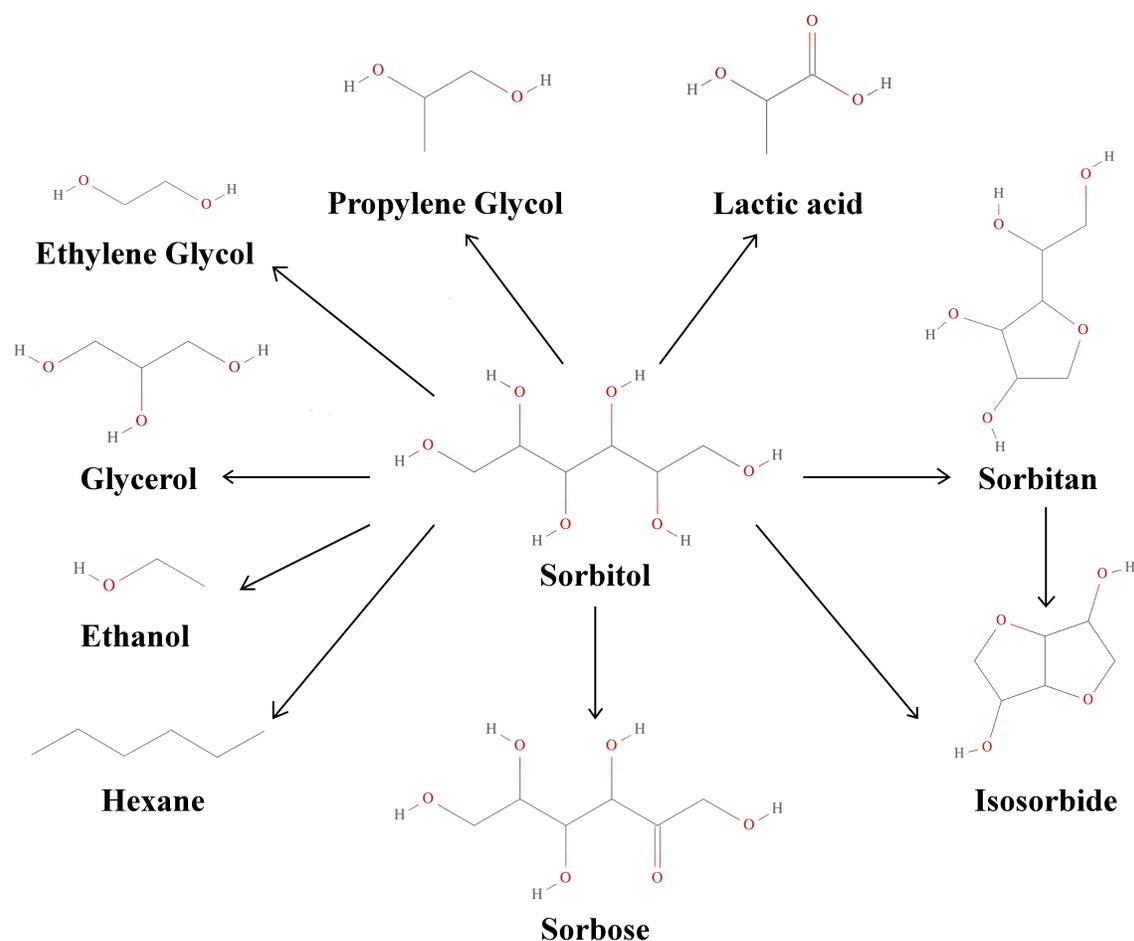
Figure 1-7. Derivative chemicals from sorbitol.[92,93]

1.6 Summary of following chapters

The scope of this dissertation is to describe the catalytic performance for the hydrolytic hydrogenation of cellulose of a series of metal oxides comprised from one up to three mixed metal oxides, metal oxides with their surface functionalized with phosphate cations and zeolites.

Chapter 2 presents the methodology used for the experiments. It also presents the materials, the procedures for the synthesis of binary and ternary metal oxides, phosphate materials and ruthenium deposition as metal functionality. Moreover, it includes a description of the characterization techniques, as well as the parameters and procedures used for the

characterization. Additionally, it summarizes the procedures and parameters used, to change the crystallinity of cellulose, to study the hydrothermal stability of the catalysts and the reaction conditions.

The studies of the catalytic performance of the metal oxides for the conversion of microcrystalline cellulose are presented in Chapter 3. The single metal oxides studied with and without ruthenium were SiO_2, Al_2O_3, TiO_2, ZrO_2, MgO, Nb_2O_5 and hydrated Nb_2O_5 (HY 340). Binary and a ternary metal oxide, also were investigated with and without ruthenium, like fumed SiO_2-TiO_2, Al_2O_3-TiO_2, Fe_2O_3-TiO_2, and synthesized by the sol-gel technique: SiO_2-TiO_2, WO_3-TiO_2, SiO_2-TiO_2-WO_3. Finally, this chapter presents the characterization results obtained for these materials and a study of the effect of temperature and time on the conversion of ball-milled cellulose with Ru/SiO_2-TiO_2-WO_3.

Chapter 4 presents the catalytic performance of the phosphate metal oxide materials during the hydrolytic hydrogenation of ball-milled cellulose. A series of studies are presented in this chapter relative to the catalytic performance of commercial crystalline niobium phosphate ($NbOPO_4$ B1), amorphous niobium phosphate ($NbOPO_4$ B2), and $NbOPO_4$ B3, $TaOPO_4$ B1 and $TaOPO_4$ B2 synthesized in our laboratory, with and without ruthenium deposition. A study of the effect of surface functionalization of the niobium oxide with the addition of phosphate is investigated to understand the relationship of this cation with acidity and how the acidity influences the catalytic performance. Additionally, the effects of cellulose crystallinity, cellulose to catalyst ratio, reaction temperature and reaction time were also studied. The effect of the addition of phosphoric acid to mesoporous materials like Ru/SBA-15, Ru/CMK-3, and non-porous materials like Ru/C and Ru/Nb_2O_5 (HY 340), was also studied to compare with the behavior of phosphates leaching from the niobium phosphate and behaving as an acid in solution.

Finally, hydrothermal stability treatments were performed to the phosphate materials at different temperatures and times, to study its stability.

The characterization and the catalytic performance for the conversion of ball-milled cellulose for zeolites like LS-USY and a titanium silicate material called UPRM-5 with and without ruthenium as metal functionality are presented in Chapter 5. Finally, concluding remarks of this work are summarized in Chapter 6.

2 METHODOLOGY

This chapter presents the methodology used for experimentation i.e., the materials, the procedures for synthesis and metal deposition, the characterization techniques and their parameters. Additionally, the procedures and parameters used for cellulose treatments, hydrothermal stability treatments and the reaction conditions used.

2.1 Materials

Microcrystalline cellulose was used as primary source of biomass and was purchased from Alpha Aesar. The single metal oxide catalysts: zirconium dioxide (ZrO_2), aluminum oxide (Al_2O_3), amorphous fumed silicon dioxide (SiO_2), P25 titanium dioxide (TiO_2) were obtained from Degussa Corp. Additional single metal oxides studied include magnesium oxide (MgO, 99.99%, extra pure, Acros Organics) and niobium (V) oxide (Nb_2O_5, 99.99%, Acros Organics). Also from Degussa Corporation we used SiO_2-TiO_2 (F 289, 8% SiO_2), Fe_2O_3-TiO_2 (F405, 6-8% Fe_2O_3) and Al_2O_3-TiO_2 (Al-Ti F 326). Furthermore, the ion exchange resin amberlyst (A-15, Sigma Aldrich), low sodium ultra stable zeolite Y (LS-USY, Grace) and tetrabutylammonium titanium silicate (TBA-UPRM-5) were also studied. For the details of TBA-UPRM-5 synthesis please refer to the literature.[111] Tetraisopropyl titanate (TYZOR TPT, Dupont), Tetramethoxysilane (TMOS, Fluka) and Tungsten VI isopropoxide 5% w/v n-isopropanol (W[OCH(CH3)2]6, Alfa aesar) were used as titanium, silicon and tungsten oxide precursors for the preparation of the SiO_2-TiO_2, WO_3-TiO_2 and SiO_2-TiO_2-WO_3 using sol-gel methods. Additionally, 2-propanol HPLC grade (Fisher, 99.9%), HCl (Fluka, 37%) and Phosphoric acid (H_3PO_4, 85%, Acros Organics.) were also used.

The niobium catalysts: niobic acid (Nb_2O_5 HY 340), two different niobium phosphates ($NbOPO_4$) named B1 (crystalline) and B2 (amorphous), were supplied from Companhia Brasileira de Metalurgia e Mineracão (CBMM). For the phosphate catalysts preparation, L(+)-Tartaric acid (ACS reagent) and ammonium phosphate dibasic (99+%) were obtained form Acros Organics. Ethanol (200 proof, anhydrous, 99.5%) and hexadecyltrimethyl ammonium bromide (CTAB, 98%) were supplied from Sigma Aldrich. The niobium (niobium (V) ethoxide, 99.9+%Nb) and tantalum (tantalum (V) ethoxide, 99.9+%Ta) precursors were purchased from Strem Chemicals.

2.2 Catalyst preparation

2.2.1 Synthesis of binary and ternary metal oxide catalysts

The binary and ternary metal oxides studied were synthesized by Rafael Méndez-Román[112] using the sol-gel method adapted from the methodology presented by Anderson and Bard.[113] The acid catalyzed hydrolysis of SiO_2-TiO_2 catalysts was conducted by mixing tetramethoxysilane (TMOS) and tetraisopropyl titanate (TYZOR) in a ratio that gave 15%w of SiO_2 in a glove box for about 20min. TMOS-TYZOR solution was added dropwise to 250mL of 2-propanol HPLC grade and 1mL of concentrated HCl solution that was stirred at 273K in an ice bath. Water at 273K was added dropwise to this final solution with vigorous stirring until the gelation process began. Then, the precipitate was aged at room temperature for 24h. The remaining solvent was removed in a vacuum oven for 48h at 310K. The final solid material was calcined in an air atmosphere at 673K for 5 days. WO_3-TiO_2 and SiO_2-TiO_2-WO_3 samples were prepared by the same process used for the SiO_2-TiO_2 sample. For the WO_3-TiO_2 catalyst, tungsten VI isopropoxide 5% w/v n-isopropanol was used as the tungsten oxide precursor and with a

proportion of tungsten oxide-titania of 25%w of WO_3. For the ternary oxide sample, the three precursors mentioned above were used with a 9.1%/81.8%/9.1%w proportion of silica-titania-tungsten oxide.

2.2.2 Synthesis of tantalum and niobium phosphate catalysts

The phosphate materials were prepared according to the synthesis described by Jiménez–Morales et al.[114] A tartrate complex was prepared by mixing the tartaric acid; previously dissolved in ethanol with the niobium or tantalum precursor at a molar ratio of 3. Then, the complex solution was evaporated until just before precipitation (a sample of tantalum tartrate was left to start to precipitate, called $TaOPO_4$ B2). After evaporation of the solvent, water was added to the complex at room temperature with a complex:water molar ratio of 0.005684 and left stirring for approximately 0.25 h. Ammonium phosphate dibasic, dissolved previously in deionized water at a ratio equal to 0.03894, was added to the complex solution with a molar ratio of 2.52 and left stirring. Hexadecyltrimethyl ammonium bromide (CTAB) was used as a structure-directing agent. It was dissolved previously in deionized water with a molar ratio equal to 0.0046. The CTAB solution was added to the previous solution with a CTAB:Complex ratio of 0.3201 with vigorous stirring for 0.5 h. After that, the white precipitate was placed in a teflon autoclave to anneal at 403 K for 24 h. The solid obtained was filtered and washed with distilled water until constant pH, it was finally washed with 200 mL of ethanol, left to dry overnight and placed in an oven to dry at 333 K for 24 h. The dried solid was calcined in air at 823 K for 6 h to eliminate the structure-directing agent.

2.2.3 Ruthenium deposition

Ruthenium was deposited on the supports using ruthenium (III) nitrosyl nitrate solution $(Ru(NO)(NO_3)_3$, 1.5%Ru, Strem Chemicals) using evaporative deposition with a nominal ruthenium loading of 4% by weight. For SiO_2, we also prepared a sample with 10% ruthenium loading. To increase the volume of the suspensions we pour slowly 30 mL of DI water. The suspension was heated to 313 K with continuous stirring until dry. The resulting material was dried for 12 h under vacuum in an oven at 373 K. Before reaction, the catalysts were reduced with a hydrogen flow of 100 mL min^{-1} using a temperature ramp of 1 K min^{-1} from room temperature to 723 K, followed by a constant temperature heating for 2 h. The samples were cooled down to room temperature after the treatment in a helium flow of 100 mL min^{-1} using a temperature ramp of 3.5 K min^{-1}. The ruthenium loading was characterized by elemental analysis at Galbraith Laboratories using Inductively Coupled Plasma (ICP).

2.3 Characterization techniques

The BET method was used to determine the surface area of the catalysts by nitrogen adsorption at 77 K, using a Micromeritics ASAP 2020 volumetric porosimetry test instrument with a turbo-molecular drag pump. Prior to each nitrogen adsorption measurement, the catalysts were degassed under vacuum for 5 h at 363 K with a heating rate of 10 °C min^{-1}.

Characterization with X-ray diffraction (XRD) was used to determine the crystalline phases present in the samples. For this technique, we used a Rigaku Ultima III diffractometer with Cu Kα target ($\lambda = 1.5418$ Å) operating at 40 kV and 44 mA. XRD patterns were collected in the 2θ range from 20° to 70° with a scanning rate of 2.00 °/min and a step size of 0.02°, respectively.

The crystallite size of the materials was determined using the Scherrer equation.[115] This equation relates the mean crystallite size with the broadening at the full width of the half maximum (FWHM) of the intensity. The data used to make the calculations are shown in Appendix A.

$$L = \frac{K \cdot \lambda}{\beta \cdot cos\theta}$$ (2.1)

where,

L	= average crystallite size	$[nm]$
K	= shape factor	0.9
λ	= X-ray wavelength	$[nm]$
β	= broadening at FWHM intensity	$[radians]$
θ	= Bragg angle	$[radians \; or \; degree]$

The cellulose crystallinity index (CI) was calculated using the Segal method,[116] that relates the ratio of the differences between the intensity of the crystalline peak (I_{002}) and the amorphous peak (I_{am}) to the crystalline intensity obtained from the diffraction pattern.

$$CI = \frac{I_{002} - I_{am}}{I_{002}}$$ (2.2)

Infrared spectroscopy of pyridine adsorption was used to determine the type of acidity present on the samples. The main region of interest was from 1400 to 1650 cm^{-1}, since this region contains the frequencies of coordinated pyridine, pyridinium ion and H-bonded pyridine. The samples were prepared using a press (Carver, model C S/N 41000-002) where approximately 20 to 50 mg of solid was placed in a die (Carver No. 3619) with an internal diameter of 13 mm to form a circular pellet at a pressure of about 15,000 psi. The background spectrum without sample was collected at 303 K after treating the cell at 473 K for 1 h with

flowing helium to remove humidity in the chamber. A spectrum at room temperature was collected for the clean surface after heating to 623 K for 1 h in helium. The adsorption of pyridine (E.M. Science, 99.92% purity) occurs by passing a stream of helium saturated with pyridine over the catalysts through a cell at 473 K for 1 h. The pyridine saturator was placed in a constant temperature (273 K) bath to produce a vapor pressure of 4.8 Torr. Gas phase pyridine and pyridine weakly adsorbed were removed overnight by flowing 100 mL/min helium at 473 K through the cell, then cooled to room temperature and the spectrum was collected using a Nicolet 6700 Fourier Transfer Infrared Spectrometer.

The concentrations of Brønsted and Lewis for the catalyst tested were calculated using the Beer-Lambert Law equation.[117] This equation relates the adsorption of light with the properties of the material.

$$A = \frac{\varepsilon \cdot W \cdot C_w}{S} \qquad (2.3)$$

where,

A	= IR absorption intensity area		$[cm^{-1}]$
ε	= integrated molar extinction coefficient		$[cm \cdot \mu mol^{-1}]$
W	= weight of disk		$[mg]$
C_w	= weight-based concentration		$[mmol \cdot g]$
S	= sample disk area		$[cm^2]$

The integrated molar extinction coefficients obtained from an average of metal oxides from Tamura $et\ al.$ are $\varepsilon_L = 1.73\ cm \cdot \mu mol^{-1}$ and $\varepsilon_B = 1.23\ cm \cdot \mu mol^{-1}$,[117] and from Datka $et\ al.$ are $\varepsilon_L = 1.11\ cm \cdot \mu mol^{-1}$ and $\varepsilon_B = 0.73\ cm \cdot \mu mol^{-1}$ obtained from measurements of pyridine absorbed in Al_2O_3 and HY zeolite,[118] for the bands at 1440 cm^{-1} corresponding to the

vibration of the pyridine ring on Lewis (LPY) acid site and at 1540 cm^{-1} for adsorbed pyridine on Brønsted (BPY) acid. The data used to make the calculations are displayed in Appendix B.

X-ray photoelectron spectroscopy (XPS) was used to find the elemental atomic concentrations on the surface of the samples. Measurements were made using a PHI 5000 Versa Probe II with Al Kα radiation source and pass energy of 187.850 eV. A survey spectrum was run for three regions in each sample at a resolution of 0.8 eV per step. High resolution was used (0.2 eV) when the spectrum was run in the selected region of the sample.

STEM characterization was used to obtain the micrographs of the samples. The images were collected in a FEI Titan STEM with CEOS probe aberration corrector. The equipment was operated at 200 kV and with a high angle annular dark field "Z-contrast" STEM used as imaging mode for which the collection angles were 67 to 337 mrad. The CEOS probe was operated at a convergence angle of 24.5 mrad and with a current of approximately 100 pA that result in a spatial resolution of approximately 0.1 nm.

2.4 Cellulose ball-mill treatment

The crystallinity of the cellulose (Alpha Aesar) was decreased using a Spex SamplePrep 8000M Mixer/Mill with a hardened 440C stainless steel vial of 2 ¼ in diameter and 3 in of length. Two stainless steel balls of ½ in were loaded to the vial with 2 g of dried microcrystalline cellulose, the milling process was run for 100 min. Afterwards, the treated cellulose was characterized using XRD. The particle size distribution of treated cellulose was obtained using Laser Diffraction with a Malvern Instrument model IDC2000.

The mean diameter and the standard deviation of the cellulose particles before and after treatment were calculated using a particle size distribution function.[27] The mean residence

particle diameter was calculated using the data that is shown in Appendix C. The mean residence

particle diameter expression is defined by

$$D_m = \int_0^\infty D \cdot E(D)dD \qquad (2.4)$$

where,

D_m	= mean residence particle diameter	$[\mu m]$	
D	= particle diameter	$[\mu m]$	
$E(D)$	= particle size distribution function	$\dfrac{V(D)}{\int_0^\infty V(D)dD}$	
$V(D)$	= cumulative volume as function of particle diameter	$[\%V]$	
$\int_0^\infty V(D)dD$	= area under the curve for the populations of the particle size distributions	$[\mu m \cdot \%V]$	

Additionally, the standard deviation was also calculated for the cellulose particles before

and after ball-mill treatment, using the same data that is shown in Appendix C. The standard

deviation is taken from the square root of the variance. The square standard deviation or variance

equation is defined as

$$\sigma^2 = \int_0^\infty (D - D_m)^2 E(D)dD \qquad (2.5)$$

which the square term can be expanded and reduced to

$$\sigma^2 = \int_0^\infty D^2 E(D)dD - D_m^2 \qquad (2.6)$$

2.5 Catalytic performance

2.5.1 *Batch reactor*

The catalytic tests for the cellulose conversion were carried out in a 100 mL high-pressure reactor model 4793 Parr Instrument. Before reaction, the support and the cellulose were dried under vacuum for 2 h at 373 K. If a supported Ru catalyst was studied, it was reduced overnight in a hydrogen flow of 100 mL min^{-1} for 2 h at 723 K. For an experiment, cellulose (Alfa Aesar, microcrystalline or ball-milled) was placed in the reactor with approximately the amount of catalyst corresponding to 4 mmol of metal for reactions with supported Ru catalysts and the equivalent amount of support for reactions without metal. 50 mL of deionized (DI) water previously treated with helium to remove dissolved CO_2 and obtain an initial pH around 7.0, were loaded to the reactor. Figure 2-1 presents the diagram for the reaction system, the mixture inside the reactor was treated with a helium flow of 100 mL min^{-1} for 1 h under vigorous stirring, followed by low-pressure hydrogen flow of 100 mL min^{-1} for 1 h. Later on, the reactor was pressurized to 35 bar of hydrogen and rapidly heated to the desired reaction temperature (483 K in about 15 min; 503 K in approximately 17 min) using a preheated mantle and the temperature was held constant for the reaction time. The temperature was measured with a type J thermocouple (Omega) and controlled with an Omega CN9000 series type temperature controller and coupled to a 300 W heating mantle. After, the desired time, the reaction was stopped by promptly cooling the reactor in an ice-water bath.
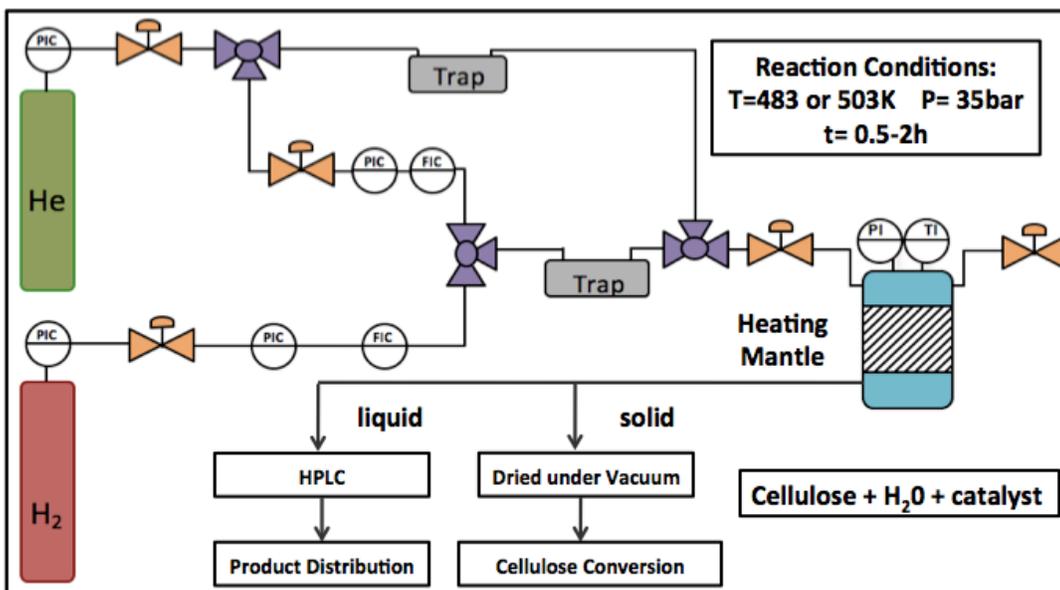
Figure 2-1. Schematic diagram for the reaction system with a batch reactor.

The liquid phase was analyzed using a High Performance Liquid Chromatography system (Waters 600 HPLC with a Waters 2410 Refractive Index Detector and a Waters 717 plus autosampler) using a carbohydrate column (Alltech 700 CH; 300 mm x 6.5 mm i.d.) with a MilliQ water mobile phase at a flow rate of 0.5 mL min^{-1} and a column temperature of 363 K. The remaining solid was filtered using a nitrocellulose filter and dried in a vacuum oven at 373 K. The conversion was calculated based on the initial cellulose weight and the cellulose recovered after the experiment, which is calculated based on the difference between the solid recovered and the amount of catalyst used $\left(m_{cellulose} = m_{solid\ recovered} - m_{catalyst}\right)$ as follows:

$$X_{cellulose} = \frac{m_{cellulose_0} - m_{cellulose}}{m_{cellulose_0}} \qquad (2.7)$$

The quantification of the products was based on their yields, which were calculated using the molar amount of cellulose in the starting material ($n_{substrate}$), the molar amount of product

$(n_{product})$ obtained by the HPLC, the stoichiometric coefficients of the cellulose $(\nu_{substrate})$ and the product $(\nu_{product})$. The stoichiometric coefficient used for cellulose is equal to one for a unit of cellulose as starting substrate. The yield equation reads as follows:[81]

$$Y_{product} = \frac{n_{product}}{n_{substrate_0}} \frac{\nu_{substrate}}{\nu_{product}} \tag{2.8}$$

The graphical representation for the yields is based on the sum of the products obtained. The yield for sugars represents glucose, fructose, arabinose and cellobiose. Furfural and 5-hydroxymethylfurfural are included in the yields of furfurals. Sorbitol and arabitol represents sugar alcohols or hexitols. Finally, the yields for glycerol, erythritol and ethylene glycol are included in the yield for hydrogenolysis products.

2.6 Hydrothermal stability

The stability in water of transition metal (V) phosphate, and Ru/Nb_2O_5 (HY 340) were investigated using a hydrothermal treatment. The stability treatments were conducted at 35 bar of H_2, two different temperatures (483 K and 503 K) and treatment times of 24 h and 48 h in a 100 mL high-pressure reactor model 4793 Parr Instrument with 50 mL of treated DI water to 0.5 g of catalyst. After treatment, the samples were filtered, rinsed with DI water until a constant pH was obtained, dried at room temperature overnight and then at 373 K for 24 h. The filtered solids were analyzed using powder X-ray diffraction, nitrogen adsorption, pyridine adsorption, X-ray photoelectron spectroscopy and inductively coupled plasma spectroscopy.

3 METAL OXIDES AS SUPPORTS FOR THE CATALYTIC CONVERSION OF CELLULOSE

The studies of the catalytic conversion of microcrystalline cellulose for the ruthenium supported on single, binary and ternary metal oxides are presented in this chapter. We also present the characterization results and a study of the effect of temperature and time on the conversion of ball-milled cellulose over Ru/SiO_2-TiO_2-WO_3.

3.1 Introduction

Metal oxides are composed of metal cations covalently or ionic bonded to oxygen atoms (Table 3-1). The differences in oxidation state of the metal oxides give differences in acidity and acid strength, important factors for the hydrolysis activity. These materials have optical, catalytic and electronic properties, useful in the petrochemical, environmental and chemical industries.[119,120] Metal oxides have many applications as heterogeneous catalysts, such as precursors, catalysts and supports.[120,121] Properties like the oxidation state of the metal cations, the crystal plane exposed of the atoms, reduction and oxidation reactions running simultaneously on the surface during reaction and their acidity (Brønsted or Lewis), makes metal oxides useful for reactions such as oxidation, dehydration, dehydrogenation, polymerization and many more.[122,123]

Table 3-1. Tentative summary of the acid-base properties of binary metal oxides.[120]

Element	Oxidation State	Cation size (radius, Å)	M-O bond nature	Acidity type	Acidity strength	Basicity, nucleophilicity	Examples
Semi-metal	$\geq^+5$	Very small ≤ 0.2	Covalent	Brønsted	Medium strong	None	$(SO_3); P_2O_5$
	$^+3-^+4$	Small ≤ 0.4	Covalent	Brønsted	Medium weak	None	B_2O_3, SiO_2, GeO_2
Metal	High $^+5-^+7$	Small to medium 0.3-0.7	Largely covalent	Brønsted and Lewis	Medium to strong	None	WO_3, MoO_3, CrO_3 Ta_2O_5, Nb_2O_5, V_2O_5
	Medium $^+3-^+4$	Small 0.35-0.5	Ionic	Lewis	Strong	Weak	γ -Al_2O_3, β-Ga_2O_3
		Medium 0.5-0.6		Lewis	Medium	Medium Weak	TiO_2, Fe_2O_3, Cr_2O_3
		Large 0.7-1.2		Lewis	Medium weak	Medium strong	$La_2O_3, SnO_2, ZrO_2,$ CeO_2 $ThO_2 (Bi_2O_3, Sb_2O_3)$
	Low $^+1-^+2$	Large to very Large 0.7-1.5		Lewis	Medium to very weak	Strong to very strong	$MgO, CaO, SrO,$ BaO, CoO $NiO, CuO, ZnO,$ (Cu_2O)

Source: Data from Shannon, R.D. and Prewitt, C.T. Acta Cryptalogr. 1969, B25, 925.

Layered transition metal oxides ($HNbMoO_6$) with inherent surface acidity showed high activities during the hydrolysis of cellulose, cellobiose, starch and sucrose attributed to the strong acidity in the gallery.[52] The dependency between the acidity and hydrolysis was shown in the conversion of cellulose to glucose over γ-Al_2O_3 and SiO_2.[14] Moreover, the use of phosphated niobium oxide was also studied for the dehydration of fructose. The modification helped to obtain higher activities than niobium oxide, thanks to the strength of acid sites on this catalyst.[53] The hydrogenation of cellulose has been studied, using different solid catalysts with the incorporation of a metal functionality.[10,12,13,18–20,67,68] Platinum on niobium-based supports were studied for the production of alkanes from biomass derived carbohydrates.[106] Nickel-promoted W-SiO_2-Al_2O_3 catalysts and Ni/γ-Al_2O_3, were studied for the hydrogenation of cellulose, and it was observed that the yield of polyols was affected by the transition metal used and the loading of this metal.[72,73] Additionally, Pt-SnO_x/Al_2O_3 was used for the conversion of cellulose to polyols and it was demonstrated that the atomic ratio of Sn/Pt affect the hexitols yields.[74] A nickel phosphide catalyst supported on SiO_2 produced high values for conversion and sorbitol

yields, due to the leaching of phosphoruos.[124] Other supports studied with transition metals were SiO_2, Al_2O_3 and MgO. Ruthenium gave the highest sorbitol yield of all the metals studied.[67] Arenesulfonic acid-functionalized mesoporous silica supported ruthenium catalyst has also been studied for the catalytic conversion of cellulose into sugar alcohols.[23] They proposed that the acid loading on the mesoporous silica support promotes the activity and the metal functionality controls the selectivity towards sugar alcohols. The disadvantage of these functionalized supports is that the sulfonic acid is not stable in hot water and is readily lost into the aqueous solution behaving as a mineral acid that attacks the cellulose and causes an apparent increase in heterogeneous catalytic activity.

The main disadvantage of metal oxides used as supports for reactions in hot water is their poor hydrothermal stability that promotes leaching, collapse or changes in the crystalline structure and loss of surface area.[23,82–84] Davis and coworkers observed a significant growth of the metal particles for Ru/γ-Al_2O_3 and Ru/SiO_2 after hydrothermal treatment at 473 K.[82] Additionally, niobium oxide is not hydrothermally stable in water at high temperatures. A study of amorphous Nb_2O_5 (HY 340) displayed a crystalline phase change and in this case, the addition of silica enhanced the stability of this material.[83] Recently, niobium oxide was used to stabilize the structure of the mesoporous silica framework; the hydrothermal stability was improved on this composite material by the formation of Nb-O-Si linkages during synthesis.[66] On the other hand, a higher stability for Pt/γ-Al_2O_3 was encountered when sorbitol or ethylene glycol were used instead of water.[125] Also, after hydrothermal treatment, there was a transformation of crystal structure from γ-alumina to boehmite.[84] Moreover, the stability of silica and γ-alumina was investigated by Pham *et al.*, improving the stability for these supports in water by adding carbon coatings on the surface of these materials.[85]

3.2 Results and discussion

3.2.1 Single metal oxides

3.2.1.1 Characterization results

The surface areas obtained for the catalysts studied are summarized in Table 3-2. The metal oxides with the lowest surface areas were the cubic structure of MgO and the pseudo-hexagonal Nb_2O_5 (Figure 3-1(a)),[126,127] displaying surface areas of 7 and 9 m^2 g^{-1}, respectively. In comparison, amorphous Nb_2O_5 (HY 340) had a surface area of 141 m^2 g^{-1}, that decreases to 71 m^2 g^{-1} with the addition of ruthenium. Additionally, for samples containing amorphous SiO_2, high surface areas were found even with the addition of ruthenium with different loadings. Furthermore, it should be emphasized that after the addition of 11.2 wt% of ruthenium to this amorphous support a peak around 44.0° appears in the diffractogram corresponding to the diffraction of the (1 0 1) plane of ruthenium with an estimated size of 24 nm as seen in Table 3-2, while for the sample with the lower ruthenium loading on SiO_2 the XRD results do not display a pattern for crystalline ruthenium as seen in Figure 3-1(b).[128–130] This probably means that the ruthenium particles are smaller than the resolution for the XRD method. Instead, for the ion-exchange resin (A-15) the XRD patterns correspond to the zero-valent ruthenium metal after reduction with a crystallite size of approximately 6 nm.[130] Furthermore, depositing ruthenium on the catalyst surfaces produces a decrease in the surface area for most of the metal oxides that indicates the low hydrothermal stability of these materials.

Table 3-2. Physico-chemical properties of catalyst samples studied.

Samples	Ru loading (wt%)[a]	Ru crystallite size (nm)[b]	S_{BET} (m^2 g^{-1})[c] Support	S_{BET} (m^2 g^{-1})[c] Ru/Support
MgO	4.59	19	7	20
ZrO_2	4.12	16	36	46
TiO_2	3.95	16	49	42
Nb_2O_5	4.41	13	9	10
Nb_2O_5 (HY 340)	4.40		141	71
Al_2O_3	5.08		99	95
SiO_2	5.65		175	178
SiO_2	11.2	24	175	167
$NbOPO_4$ B1	4.61	15	140	121
A-15		6	35	
SBA-15[d]	4.53		672	772
C[d]	4.69			935

[a]Determined by Galbraith Laboratories using ICP.
[b]Determined using the Scherrer equation.[115]
[c]Surface areas were obtained using the BET method.
[d]Data obtained from the work of Reyes-Luyanda et al.[23]
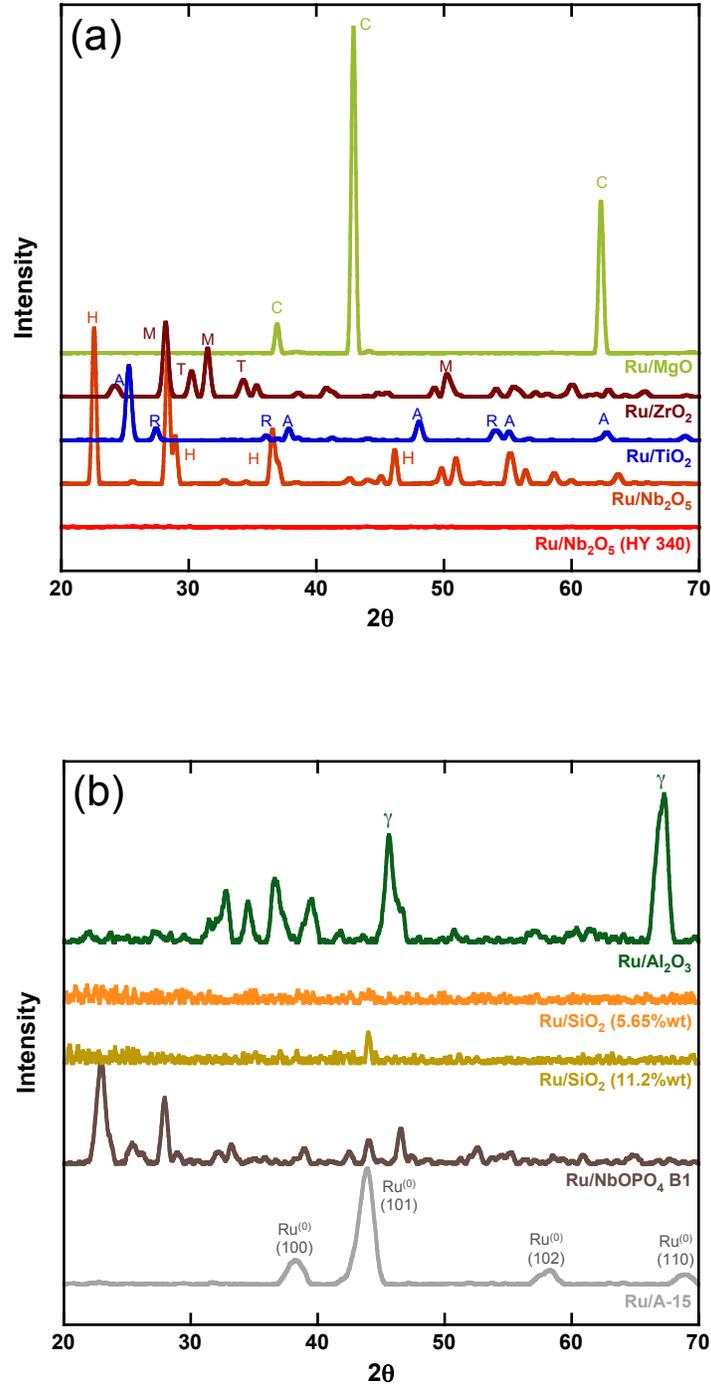
Figure 3-1. X-ray diffraction patterns of (a) Ru/MgO, Ru/ZrO₂, Ru/TiO₂, Ru/Nb₂O₅, Ru/Nb₂O₅ (HY 340), and (b) Ru/Al₂O₃, Ru/SiO₂ (11.2 wt%), Ru/NbOPO₄ B1, Ru/A-15. The crystal structures presented are cubic (C),[126] monoclinic (M),[131] tetragonal (T),[131] anatase (A),[132] rutile (R),[132] pseudohexagonal (H),[127] and gamma (γ),[84] zero-valent Ru metal (Ru$^{(0)}$).[130]

3.2.1.2 *Effect of the support acidity on the catalytic performance using microcrystalline cellulose*

Table 3-3 summarizes the results obtained for the conversion of microcrystalline cellulose using different metal oxides supports at 483 K, 35 bar of H_2 and 1 h of reaction. The conversion of these materials was compared with the results obtained for the reaction in the absence of a catalyst. The reaction occurs without a catalyst with a conversion of 24%. Under our reaction conditions the ionization constant of water is over 500 times higher than at room temperature.[133] As a result the higher hydronium ion concentration in solution at 483 K and 35 bar is responsible for increasing the solution acidity that promotes the hydrolysis of cellulose. Additionally, formic and levulinic acids are formed from the rehydration of HMF that leads to a further increase in the acid concentration, as seen in a decrease of the solution final pH, which results in an autocatalytic effect.[23]

Figure 3-2 shows the cellulose conversion as a function of the Sanderson electronegativity, of the metal oxide catalysts. The electronegativity of the metal oxide is a property that provides a measure of the surface acidity.[134] The electronegativity of the metal oxides was calculated using the Sanderson electronegativity (S_{int}) for the compound using the relationship,[135]

$$S_{int} = \left(\prod_i S_i^{p_i} \right)^{\frac{1}{\Sigma_i p_i}},$$ (3.1)

where, S_i represents the electronegativity and p_i the stoichiometric coefficient of the element i on the oxide, as tabulated in Table 3-4.[136,137]

The conversion for the supports displays a volcano shaped curve, were the highest value corresponded to Nb_2O_5 (HY 340), indicating that this material has a good catalytic performance for cellulose hydrolysis at our reaction conditions. In this graph (Figure 3-2), the values on the

left end of the curve correspond to samples with predominantly basic properties and as you move to the right hand side the acidity increases passing through a maximum before decreasing. The same behavior is observed for the cellulose conversion indicating a correlation between hydrolysis activity and surface acidity. As discussed above for the results without catalyst, in the absence of a metal functionality there is significant production of carboxylic acids that increases the acidity of the solution as can be observed by the decrease in pH as the conversion increases. For the ruthenium supported catalysts we used the same electronegativities calculated for the supports. This instance there is no clear trend observed, only that the conversions for the ruthenium supported catalysts was lower and the values cluster close to the results obtained for the reaction without the presence of a catalyst. This behavior is observed because the hydrogenation of the monosacharides inhibits the formation of the carboxylic acids and the reaction is no longer autocatalytic.

The results for the catalytic performance of the catalysts based on the metal oxides were compared with those obtained for catalysts based on crystalline niobium phosphate ($NbOPO_4$ B1) and SBA-15. As observed in Table 3-3 the conversion for A-15 was the highest. This sample decomposes at our reaction conditions, and releases the sulfonic acid groups behaving as a liquid mineral acid with an equivalent concentration of 0.03%wt of H_2SO_4. On the other hand, for the supported ruthenium materials, the yields were compared with $Ru/NbOPO_4$ B1, Ru/SBA-15 and Ru/C. For all supports the addition of ruthenium causes an increase in the selectivity for sugar alcohols, but also decrease cellulose conversion. As mentioned before the metal functionality inhibits the carboxylic acid formation, as seen by the higher pH measured after reaction.

Doubling the ruthenium loading deposited on SiO_2 slightly decreases the cellulose conversion, does not change the yield towards hexitols and increases further the final pH of the

solution after reaction. The decrease in conversion is explained by the higher pH and hence lower concentration of carboxylic acids while the higher particle size explains why there was no enhancement in the hydrogenation activity. Most of the catalysts supported on the metal oxides displayed the same conversion, but significant differences in selectivities were observed as seen in Table 3-3. This behavior may be explained by the fact that the hydrolysis activity appears controlled by the hydronium ion concentration and not by the identity of the metal oxide. But when the monosacharides are formed they do interact with the metal oxides surface and react according to the respective surface chemistry.

Both SBA-15 and Ru/SBA-15 display a slight increase in conversion compared to the values obtained for the SiO_2 based catalyst. These results may be explained by the significant difference in surface areas of these materials. The results for Ru/C are similar to the results for the metal oxide catalysts and the explanation is the same as for those materials. The catalysts based on $NbOPO_4$ B1 display a significant enhancement in catalytic performance. Both conversion and yield towards hexitols increase significantly. For this reason we decided to conduct a more detailed study of these materials as described in Chapter 4.

Table 3-3. Reaction results for cellulose conversion using ruthenium supported on metal oxides.

Samples	Final pH	Conversion (%)[a]	Yield (%)[b]			
			SA	S	H	F
No catalyst	3.345	24	0	6	0	6
Ru/MgO	9.809	23	2	1	3	0
MgO	8.275	32	0	3	0	0
Ru/ZrO$_2$	3.500	23	8	1	5	0
ZrO$_2$	3.100	34	0	6	0	9
Ru/TiO$_2$	4.015	20	7	2	5	0
TiO$_2$	3.002	35	0	7	0	5
Ru/Nb$_2$O$_5$	3.631	23	5	2	4	0
Nb$_2$O$_5$	2.962	32	0	5	0	5
Ru/Nb$_2$O$_5$ (HY 340)	3.789	22	8	1	3	0
Nb$_2$O$_5$ (HY 340)	2.650	38	0	2	0	4
Ru/Al$_2$O$_3$	5.932	18	1	1	5	0
Al$_2$O$_3$	3.161	28	0	7	0	4
Ru/SiO$_2$ (5.65 wt%)	3.909	24	8	7	5	0
Ru/SiO$_2$ (11.2 wt%)	4.158	22	8	4	3	0
SiO$_2$	3.350	29	0	4	0	6
Ru/NbOPO$_4$ B1	3.534	32	18	2	4	0
NbOPO$_4$ B1	2.806	42	0	7	0	10
A-15	2.342	62	0	28	0	12
Ru/SBA-15[c]	4.180	25	8	1	1	0
SBA-15[c]	3.123	30	0	8	0	10
Ru/C[c]	4.512	21	5	0	5	0

[a]All experiments were run with microcrystalline cellulose, a cellulose to catalyst ratio of 10, a reaction temperature of 483 K, 1 h of reaction and 35 bar of H$_2$.
[b]SA= sugar alcohols, S= sugars, H= hydrogenolysis, F= furfurals.
[c]Data obtained from the work of Reyes-Luyanda *et al.*[23]
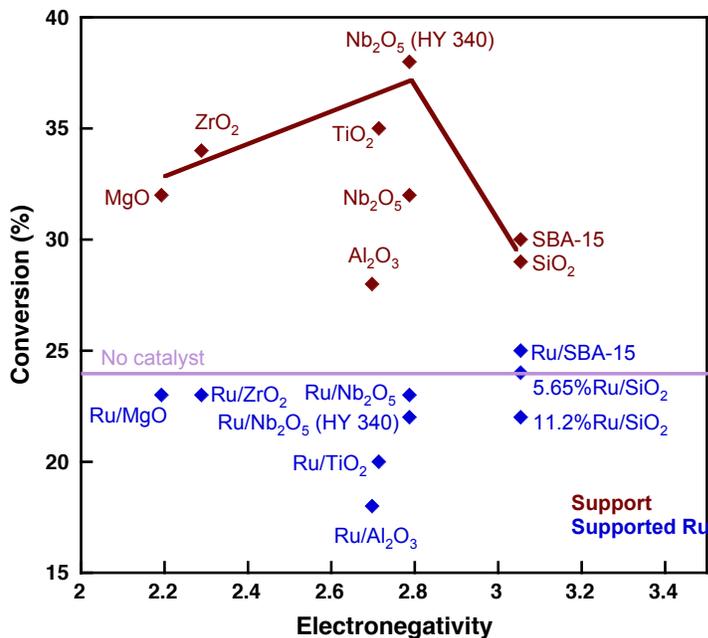
Figure 3-2. Cellulose conversion as a function of the Sanderson electronegativity for the single metal oxides. Support (♦) and supported ruthenium (♦). Reaction conditions: 483 K, 35 bar of H₂ and 1 h of reaction.

Table 3-4. Electronegativities of metal oxides.[136,137]

Element	$S_i{}^a$	Metal oxide	$S_{int}{}^b$
Mg	1.318	**MgO**	2.193
Zr	0.90	**ZrO₂**	2.289
Ti	1.50	**TiO₂**	2.714
Nb	1.42	**Nb₂O₅**	2.787
Al	1.714	**Nb₂O₅ (HY 340)**	2.787
Si	2.138	**Al₂O₃**	2.698
O	3.650	**SiO₂**	3.054

^{a}S$_i$= electronegativity of the element.
^{b}S$_{int}$= Sanderson's electronegativity calculated for the metal oxide.

39

3.2.2 Binary and ternary metal oxides

3.2.2.1 Characterization results

The surface areas for the binary and ternary metal oxides are summarized in Table 3-5 and the results display values that range from 36 to 189 m^2 g^{-1}. Furthermore, also was noticed that the addition of ruthenium to the binary and ternary metal oxide caused a decrease in the surface area for most of these metal oxides again indicating low hydrothermal stability. The diffraction patterns for the binary and ternary samples are presented in Figure 3-3. The sol-gel Ru/WO_3-TiO_2 and Ru/SiO_2-TiO_2-WO_3 present no evidence of the rutile crystal phase, only the anatase crystal structure is observed. On the other hand, Ru/SiO_2-TiO_2 (SG) shows a broad peak with low crystallinity near the intense line of the anatase pattern, consistent with the literature.[113] For Ru/SiO_2-TiO_2, Ru/Fe_2O_3-TiO_2 and Ru/Al_2O_3-TiO_2, the anatase and rutile phases were present; because the synthesis of these materials promotes the presence of both phases. Additionally, the peak at $2\theta = 44.0°$, corresponding to the (1 0 1) plane of ruthenium, was also observed for these samples,[128–130] indicating the presence of large ruthenium particles on these catalysts with crystallite sizes between 12 to 19 nm (Table 3-5).

Table 3-5. Physico-chemical properties of binary and ternary metal oxide samples.

Samples	Pyridine Concentration (μmol g^{-1})[a]		Ru Loading (wt%)[b]	Ru crystallite size (nm)[c]	S_{BET} (m^2 g^{-1})[d]	
	C_B	C_L			Support	Supported Ru
SiO$_2$-TiO$_2$ (SG)[e]	140	107	5.00	12	189	151
SiO$_2$-TiO$_2$	65	63	5.30	12	97	95
Fe$_2$O$_3$- TiO$_2$		214	5.06	19	49	36
Al$_2$O$_3$- TiO$_2$		240	7.12	14	54	56
WO$_3$- TiO$_2$ (SG)	151	96	4.77	16	66	91
SiO$_2$-TiO$_2$-WO$_3$ (SG)			4.74	15	150	116

[a]Brønsted and Lewis Concentration calculated by the expression proposed by Tamura.[117]
[b]Determined by Galbraith Laboratories using ICP.
[c]Determined using the Scherrer equation.[115]
[d]Surface areas were obtained using the BET method.
[e]SG= synthesized using a sol-gel procedure.[138]
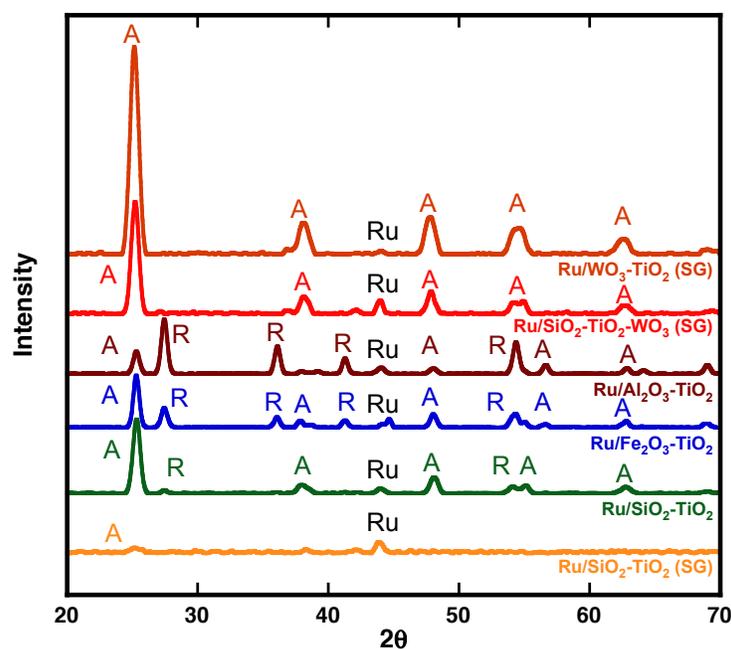
Figure 3-3. X-ray diffraction patterns of Ru/WO$_3$-TiO$_2$, Ru/SiO$_2$-TiO$_2$-WO$_3$, Ru/Al$_2$O$_3$-TiO$_2$, Ru/Fe$_2$O$_3$-TiO$_2$, Ru/SiO$_2$-TiO$_2$ (Degussa) and Ru/SiO$_2$-TiO$_2$ (sol-gel). The crystal structures include anatase (A) and rutile (R).

The acidity of the binary and ternary metal oxides was analyzed using IR spectroscopy of pyridine adsorption at 473K, as shown in Figure 3-4. The spectrum for SiO_2 shows two IR bands centered at 1446 and 1598 cm^{-1} corresponding to hydrogen bonded pyridine (Table 3-6).[112,139] For TiO_2, the four bands observed correspond to the vibrations of the pyridine ring on Lewis acid sites. When Si is incorporated into TiO_2, new bands are generated at 1544 and 1640 cm^{-1}, indicating the presence of Brønsted acid sites as seen for the sol-gel and Degussa samples. Additionally, the Lewis acid site bands are also present, but with lower intensity than for TiO_2, indicative of a decrease in Lewis acid concentration for the binary compounds. This behavior was also observed for the WO_3-TiO_2 sample. The Brønsted concentrations for sol-gel samples were 140 and 151 μmol g^{-1}, otherwise the concentration for the commercial SiO_2-TiO_2 was 54% lower than the sol-gel sample. FTIR spectra for pyridine adsorption on Fe_2O_3-TiO_2 and Al_2O_3-TiO_2 display bands appearing near 1445, 1490, 1575 and 1604 cm^{-1}, respectively that corresponds to adsorption on Lewis acid sites with concentrations of 214 and 240 μmol g^{-1} as obtained from the Beer-Lambert law (Eq. 2.3).
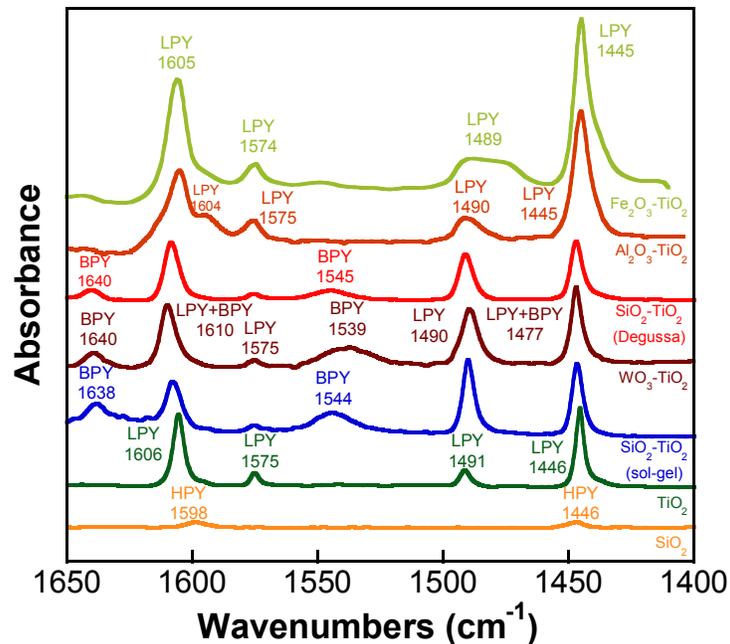
Figure 3-4. FTIR spectra for pyridine adsorption at 473 K on SiO₂, TiO₂, SiO₂-TiO₂ (SG), WO₃-TiO₂, SiO₂-TiO₂, Al₂O₃-TiO₂, Fe₂O₃-TiO₂. H-bonded pyridine (HPY), Lewis acid sites are identified with LPY, and Brønsted acid sites are identified with BPY.[112]

Table 3-6. Configuration and IR characteristics of pyridine adsorbed species on metal oxide surfaces at ≥ 300 K.[139]

Py Species	T /K	Configuration	$\nu CCN/cm^{-1}$	
			ν_{8a}	ν_{19b}
PPy	300		1585	1445 & 1435
HPy	300		1600-1580	1447-1440
BPy	300		1640-1630	1540-1500
LPy	300		1633-1600	1460-1445

>300 K OH⁻   >300 K O²⁻

$\nu C{=}O$ at 1580-1560cm⁻¹ — α−Pyridone

$\nu N^{+}{-}O$ at 1260-1250 cm⁻¹ — Pyridinium oxide
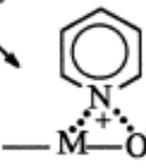
3.2.2.2 Catalytic performance for conversion of microcrystalline cellulose

Table 3-7 summarizes the results for cellulose conversion when binary and ternary metal oxide based catalysts were used at 483 K, 35 bar of H_2 and 1 h of reaction. The results for the catalysts based on binary and ternary metal oxides are similar to those described above for the single metal oxides. As it is seen in Table 3-7, SiO_2-TiO_2 catalysts and WO_3-TiO_2 (SG) display the highest cellulose hydrolysis activities with conversions between 38 and 39%. These conversions are higher than the conversions obtained for any of the catalysts based on the single metal oxides. These catalysts have Brønsted acidity and it has been shown that Brønsted acidity promotes both dehydration and rehydration reactions that yield carboxylic acids.[11,140]

Once again when ruthenium is deposited on the binary and ternary metal oxides we observed a leveling effect similar to that described above for the single metal oxides. This instance the conversions are even lower and the final pH values are higher than most of the catalysts discussed before. The Ru/SiO_2-TiO_2-WO_3 (SG) sample was the most selective for the production of hydrogenolysis products from sugar alcohols with a yield of 8%.

Table 3-7. Reaction results for cellulose conversion on binary and ternary metal oxides.

Samples	Final pH	Conversion (%)[a]	Yield (%)[b]			
			SA	S	H	F
No catalyst	3.345	24	0	6	0	6
Ru/SiO$_2$-TiO$_2$ (SG)[c]	4.125	19	6	0	2	0
SiO$_2$-TiO$_2$ (SG)	2.938	39	0	4	0	9
Ru/SiO$_2$-TiO$_2$	7.273	18	1	1	3	0
SiO$_2$-TiO$_2$	2.864	38	0	5	0	10
Ru/Fe$_2$O$_3$- TiO$_2$	5.111	17	5	1	3	0
Fe$_2$O$_3$- TiO$_2$	3.045	28	0	4	0	6
Ru/Al$_2$O$_3$- TiO$_2$	7.982	16	1	1	1	0
Al$_2$O$_3$- TiO$_2$	3.032	27	0	3	0	8
Ru/WO$_3$- TiO$_2$ (SG)	3.977	23	8	0	4	0
WO$_3$- TiO$_2$ (SG)	2.800	38	0	6	0	3
Ru/SiO$_2$-TiO$_2$-WO$_3$ (SG)	4.100	23	3	3	8	0
SiO$_2$-TiO$_2$-WO$_3$ (SG)	2.821	36	0	8	0	17
Ru/SBA-15[d]	4.180	25	8	1	1	0
SBA-15[d]	3.123	30	0	8	0	10
Ru/C[d]	4.512	21	5	0	5	0

[a]All experiments were run with microcrystalline cellulose, a cellulose to catalyst ratio of 10, a reaction temperature of 483 K, 1 h of reaction and 35 bar of H$_2$.
[b]SA= sugar alcohols, S= sugars, H= hydrogenolysis, F= furfurals.
[c]SG= synthesized using a sol-gel procedure.[138]
[d]Data obtained from the work of Reyes-Luyanda *et al.*[23]

3.2.2.3 Effect of temperature and reaction time for the ternary metal oxides in the conversion

 of ball-milled cellulose

Ruthenium supported on SiO$_2$-TiO$_2$-WO$_3$ (SG) was the only metal oxide catalyst that produced high yields for the hydrogenolysis products during the conversion of microcrystalline cellulose. Due to those results, the effects of reaction time and temperature were studied for this catalyst during the conversion of ball-milled cellulose in an attempt to optimize the reaction conditions. Those influences over the cellulose conversion and yields are displayed in Figure 3-5, Figure 3-6 and Table 3-8. The conditions studied include temperatures of 483 K and 503 K and reaction times that go from 0.5 to 2 h. For comparison purposes reactions in the absence of a

catalyst were also studied. As observed in Figure 3-5, an increase in conversion is obtained increasing the reaction temperature to 503 K, because the ionization constant of water (K_w) is 600 times the ionization constant at ambient temperature (K_w [503 K, 35 bar] > 600 K_w [298 K, 35 bar]), and therefore there is an increase in the hydronium ion concentrations as we increased the temperature that helped increase the cellulose conversion.[133]
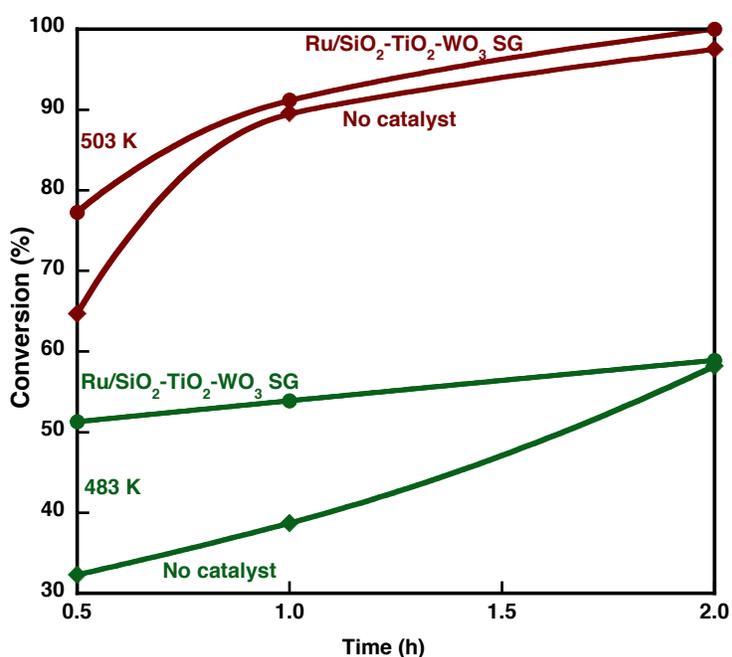
Figure 3-5. Cellulose conversion as a function of reaction time and temperature for Ru/SiO$_2$-TiO$_2$-WO$_3$ SG (circles) and the reaction in the absence of a catalyst (diamonds) with a cellulose to catalyst ratio of 3.3, 35 bar of H$_2$ and ball-milled cellulose. Temperatures of analysis were 483 K (green) and 503 K (red).

The conversion for Ru/SiO$_2$-TiO$_2$-WO$_3$ (SG) was always higher than when no catalyst was used. The difference is significantly higher when the reaction is conducted at 483 K. For 503 K the difference in conversion decreases as the reaction time increases. The yields as a function of temperature and time are illustrated in Figure 3-6. The yield towards sugar alcohols appears to go through a maximum near 1 h for both temperatures. At 483 K there is a slight increase in the yield towards hydrogenolysis products from 1 to 2 h while at 503 K it stays nearly constant at 16%. As a result, Ru/SiO$_2$-TiO$_2$-WO$_3$ (SG) appears to be a better catalyst to obtain hydrogenolysis products than for the production of sugar alcohols, as observed in their selectivity on the conversion of microcrystalline and ball-milled cellulose.
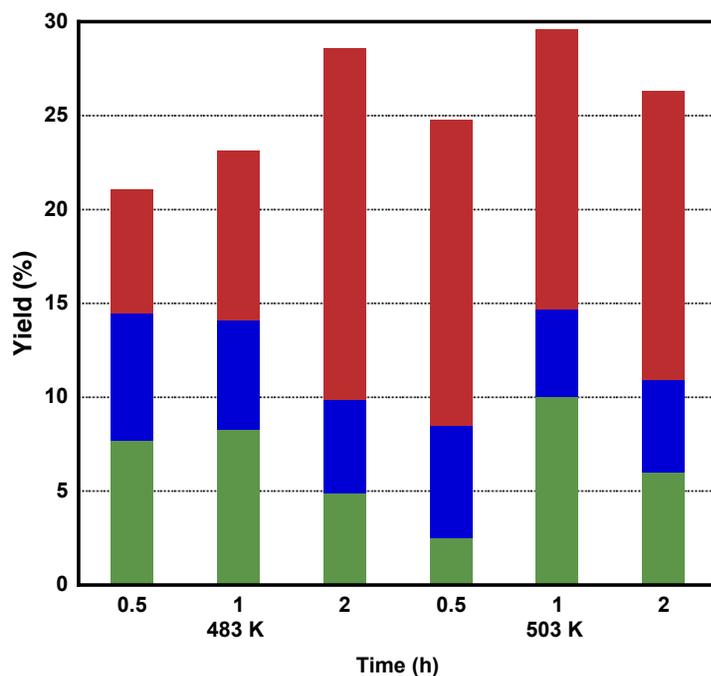
Figure 3-6. Yields as a function of reaction time and temperature for Ru/SiO$_2$-TiO$_2$-WO$_3$. Temperatures of analysis were 483 K and 503 K. Reaction times 0.08 h ≤ t ≤ 2 h. Reaction products: sugar alcohols (green), sugars (blue) and hydrogenolysis products (red).

Table 3-8. Reaction results for the cellulose conversion as a function of reaction time and temperature.

Sample	Temp. (K)	Time (h)	pH	Conversion (%)[a]	Yield (%)[b]			
					SA	S	H	F
No catalyst	483	0.5	4.039	32	0	9	0	4
		1	3.989	39	0	8	0	4
		2	3.411	58	0	4	0	5
Ru/SiO$_2$-TiO$_2$-WO$_3$ (SG)[c]	483	0.5	3.434	51	8	7	7	0
		1	3.492	54	8	6	10	0
		2	5.075	59	5	5	19	0
No catalyst	503	0.5	3.979	65	0	7	0	6
		1	3.528	90	0	7	0	10
		2	4.900	98	0	12	0	9
Ru/SiO$_2$-TiO$_2$-WO$_3$ (SG)[c]	503	0.5	4.542	77	3	6	16	0
		1	3.421	91	10	5	15	0
		2	3.460	100	6	5	15	0

[a]All experiments were run with ball-milled cellulose, a cellulose to catalyst ratio of 3.3, a reaction temperature of 483 and 503 K, 0.5, 1 and 2 h of reaction and 35 bar of H$_2$.
[b]SA= sugar alcohols, S= sugars, H= hydrogenolysis, F= furfurals.
[c]SG= synthesized using a sol-gel procedure.[138]

3.3 Conclusions

The cellulose hydrolysis catalytic activity for the single metal oxides supports correlates with the Sanderson electronegativity of the metal oxides passing through a maximum for amorphous Nb_2O_5 (HY 340). The single, binary and ternary metal oxides that have Brønsted acidity displayed higher cellulose hydrolysis activity. In both instances the apparent increase in hydrolysis activity is caused by the formation of carboxylic acids that cause an autocatalytic effect. Depositing ruthenium on all the metal oxides studied causes a marked decrease in cellulose conversion to values lower than those observed without catalyst. The addition of the metal functionality makes the reaction no longer autocatalytic, because it inhibits carbohydrate dehydration and the rehydration of furfurals. Also, it was seen that the ruthenium loading on all supports increases the selectivity towards sugar alcohols. This corroborated that having a metal surface aids the production of these polyols.

Additionally, the strong Brønsted acidity of the crystalline niobium phosphate with and without ruthenium appears to promote the hydrolysis of cellulose obtaining high conversions. Among all supports and supported ruthenium metal oxides catalysts tested, the crystalline niobium phosphate material shows the best catalytic performance for the microcrystalline cellulose conversion. An analysis of temperature and reaction time for the hydrolytic hydrogenation of ball-milled cellulose using Ru/SiO_2-TiO_2-WO_3 (SG) corroborated the same behavior observed as for the conversion of microcrystalline cellulose, in which higher yields for hydrogenolysis products were obtained than for sugar alcohols.

4 GROUP V TRANSITION METAL PHOSPHATE FOR THE HYDROLYTIC HYDROGENATION OF CELLULOSE

This chapter presents a study of the catalytic performance of two commercial niobium phosphates: crystalline niobium phosphate (NbOPO$_4$ B1) and amorphous niobium phosphate (NbOPO$_4$ B2), as well as phosphates synthesized in our laboratory: NbOPO$_4$ B3, TaOPO$_4$ B1 and TaOPO$_4$ B2 with and without ruthenium deposition, for the hydrolytic hydrogenation of ball-milled cellulose. The variables studied include the effect of phosphate functionalization of niobium oxide, the cellulose crystallinity, the cellulose to catalyst ratio, the reaction temperature and time, the addition of phosphoric acid to Ru/SBA-15, Ru/CMK-3, Ru/Nb$_2$O$_5$ (HY 340) and Ru/C, and hydrothermal treatments.

4.1 Introduction

Transition metal (V) phosphates have been used as catalysts, supports, protonic conductors, for cation mobility, for ceramic preparations, and in the optical industry as coatings, due to their similar chemical properties.[114,141–145] The metal phosphates possess properties such as the mobility of lattice oxygen and mild acid-base properties, essential for their application in oxidation reactions.[143] Additionally, it has been observed that the catalytic, acidic and textural properties of these phosphate materials are conserved at high temperatures.[146]

Furthermore, metal (V) phosphates possess high reactivity for reactions performed in water, demonstrating their stability and activity under those conditions.[56,106] The presence of water molecules on the surface of the transition (V) metal phosphates, imparts strong acidity

properties to these supports, due to the highly polarized M-OH bonds that act as Brønsted acid sites.[114,147,148] Niobic acid has an acid strength that is equivalent to having a solution of sulfuric acid with a 70% of concentration that increases with phosphoric acid treatment and is conserved with water treatment.[100,114,146,148,149]

Metal phosphates have been used as catalysts in many reactions such as the alkylation of anisole, toluene, phenol and aromatic compounds with benzyl chloride, 1-dodecene, 1-octene, 2-octanol, 1-octen-3-ol, and other alcohols.[150–156] Also, these materials have been used in the oxidation of hydrogen, methanol, benzyl-alcohol, naphtol, phenol, and the oxidative dehydrogenation of ethane.[157–162] Other reactions such as the esterification of fatty acids with alcohols, acetylation of glycerol with acetic anhydride and reforming of dimethoxymethane have used phosphate materials as catalysts.[163–165] They have also been used as proton conductors for fuel cells, and as catalysts for methanolysis of sunflower oil and the dehydration of methanol and butanol.[114,148,166–168]

In terms of biomass derived products, niobium and tantalum phosphate have been mostly used for the dehydration of glucose and fructose to 5-hydroxymethylfurfural. It was observed that the phosphate materials gave higher activities than the parent metal oxides thanks to the strength of the acid sites generated by the phosphating procedure.[53–57] Deactivation of the catalysts was observed when they were used for long periods, due to contamination by humins.[53,55,56,147] Dehydration of sorbitol to isosorbide was also studied using tantalum or niobium phosphate as catalysts.[100,169,170] Additionally, the production of hexane and octane from biomass derivatives was also studied.[106,171]

We are aware of only one study for the conversion of cellulose to sorbitol using niobium phosphate. Ru/NbOPO$_4$ was studied with different initial pHs and RuCl$_3$ as ruthenium precursor.

The authors demonstrated that the high catalytic performance of this catalyst was partly due to the high acidity of the catalyst.[70] As mentioned before, using chlorine-containing metal precursors affects the catalytic performance due to residual chlorine anions that leach into solution, increasing the acidity of solution, and eventually increasing the conversion of cellulose.[71] These chlorine ions cause an apparent improvement of the catalytic performance of this material that is not inherent to the catalyst.

4.2 Results and discussion

4.2.1 Commercial niobium phosphate

4.2.1.1 Effect of surface functionalization

The acidity of catalysts can be increased with the functionalization of the surface either with the addition of an acid functional group on the surface like sulfonic acid or with the incorporation of cations in the structure. Figure 4-1, Figure 4-2 and Table 4-1 present the results for the catalytic performance of SBA-15 functionalized with sulfonic acid groups (SBA-15S)[23] and phosphate niobia B1 compared to the parent materials and to the results without catalyst for the conversion of microcrystalline cellulose at 483 K and 1 h of reaction. As shown the addition of a catalyst without a metal functionality always increases the conversion of cellulose, when compared to the results without catalyst. A catalyst with Brønsted acidity such as Nb_2O_5 (HY 340) has higher conversion than a catalyst with neutral acidity like mesoporous silica (SBA-15). Moreover, when 0.43 mmol of sulfonic acid per g of catalyst is added to the mesoporous structure of SBA-15 the conversion increases from 30 to 51 % and the yields for sugar and furfurals also increase significantly. One problem with these materials is that they are not hydrothermally stable and the acid functionality readily leaches at our reaction conditions.

53

Phosphating Nb_2O_5 (HY 340) also causes an increase in cellulose conversion, but smaller than for SBA-15. Additionally, as observed before, the metal deposition causes a decrease in conversion and an increase in the selectivity towards sugar alcohols. As shown in Figure 4-2, the highest yield towards sugar alcohols is obtained with Ru/SBA-15S. At the reaction conditions the sulfonic acid functional groups leach into solution and behave like a mineral acid, increasing the hydrolysis of cellulose, which in turn increases the production of glucose that is converted to sorbitol over ruthenium leading to an increase in the yield of sugar alcohols.
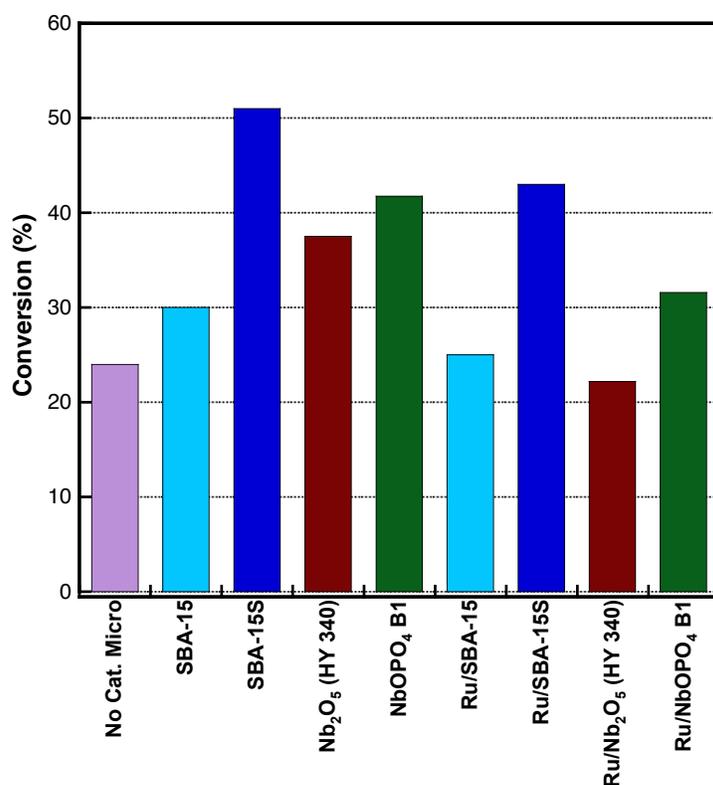

Figure 4-1. Effect of changing the surface functionalization on the cellulose conversion. The reactions were run using microcrystalline cellulose (Micro) at 483 K, 1 h, 50 mL of water, cellulose to catalyst ratio of 10 and 35 bar of H_2. Data of mesoporous SBA-15 obtained from the work of Reyes-Luyanda et al.[23]
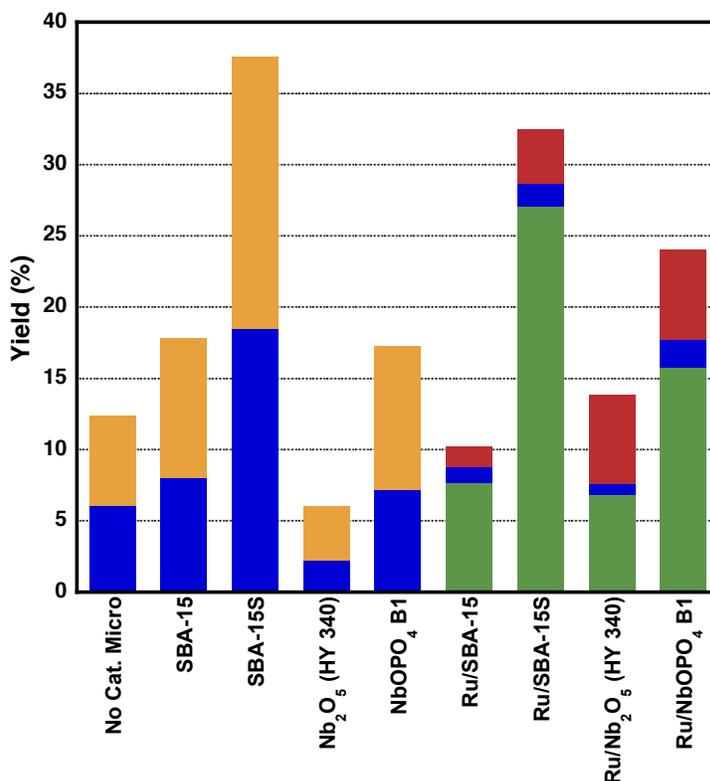
Figure 4-2. Effect of changing the surface functionalization on the yields. The reactions were run for microcrystalline cellulose (Micro) at 483 K, 1 h, 50 mL of water, cellulose to catalyst ratio of 10 and 35 bar of H_2. Reaction products: sugar alcohols (green), sugars (blue), hydrogenolysis products (red) and furfurals (yellow). Data of mesoporous SBA-15 obtained from the work of Reyes-Luyanda *et al.*[23]

Table 4-1. Reaction results for the effect of changing the surface functionalization.

Samples	Final pH	Conversion (%)[a]	Yield (%)[b]			
			SA	S	H	F
No catalyst	3.345	24	0	6	0	6
SBA-15[c]	3.123	30	0	8	0	10
SBA-15S[c]	2.850	51	0	19	0	19
Nb_2O_5 (HY 340)	2.650	38	0	2	0	4
$NbOPO_4$ B1	2.806	42	0	7	0	10
Ru/SBA-15[c]	4.180	25	8	1	1	0
Ru/SBA-15S[c]	3.220	43	27	2	4	0
Ru/Nb_2O_5 (HY 340)	3.789	22	8	1	3	0
Ru/$NbOPO_4$ B1	3.534	32	18	2	4	0

[a]All experiments were run with microcrystalline cellulose, a cellulose to catalyst ratio of 10, a reaction temperature of 483 K, 1 h of reaction and 35 bar of H_2.
[b]SA= sugar alcohols, S= sugars, H= hydrogenolysis, F= furfurals.
[c]Data obtained from the work of Reyes-Luyanda *et al.*[23]

4.2.1.2   Effect of cellulose crystallinity and cellulose to catalyst ratio

The crystallinity of cellulose has been studied by many authors and various methods have been used to decrease the crystallinity of cellulose like using mineral acids, subcritical water and ball-milling treatments.[14,70,78,172–176] Since niobium phosphate displayed good catalytic performance, we used this material to study the effect of decreasing the cellulose crystallinity on performance. The crystallinity index (CI) measures the ratio of crystalline to amorphous cellulose and is determined by the differences of crystalline to amorphous intensity divided by the intensities of the crystalline peak (Eq. 2.2).[116,177,178] Ball-milling cellulose for 1.7 h (100 min) decreases the crystallinity index from 86% to 0% as observed in Figure 4-3. Additionally, the particle size distribution gets wider after ball-mill treatment, with an increase in the number of small particles, as presented in Figure 4-4. The deconvolution of the microcrystalline particle size distribution shows two particle populations with mean diameters of 65 μm and 137 μm with a standard deviation (σ) of 59 μm and 49 μm. Instead, three populations were obtained for the ball-milled cellulose. The calculated mean diameters are 23, 65 and 171μm and the standard deviations vary from 21, 46 and 56 μm. Appendix C shows the deconvolution of cellulose materials. The deconvolution of both particle size distributions gives particles with mean diameters of 65 μm, but with lower area (260 μm) for the ball-milled cellulose than 341 μm for microcrystalline cellulose. For the ball-milled cellulose there is a new distribution corresponding to smaller particles with a mean diameter of 23 μm. the larger particle size distribution decreases significantly in intensity and the mean particle size increases somewhat probably indicating some agglomeration or preferential decrease in medium size particles.
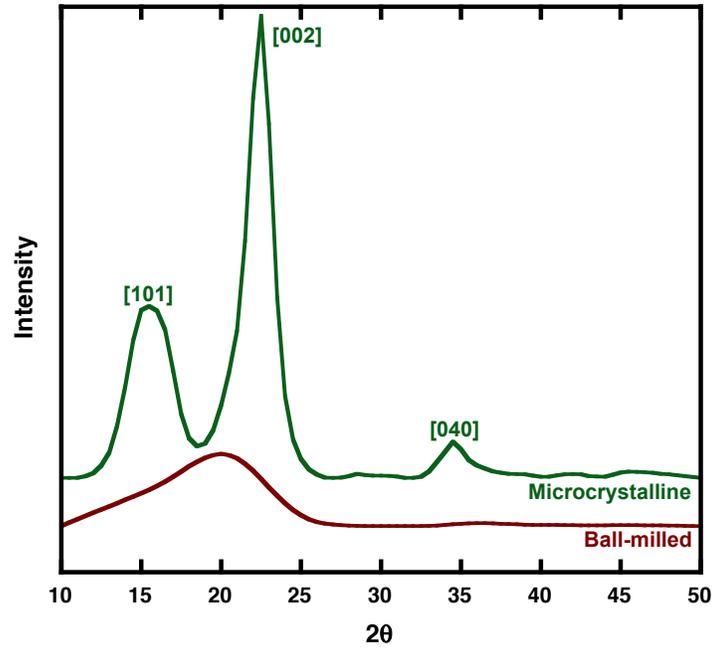
Figure 4-3. X-ray diffraction patterns of microcrystalline (green) and ball-milled cellulose (red).
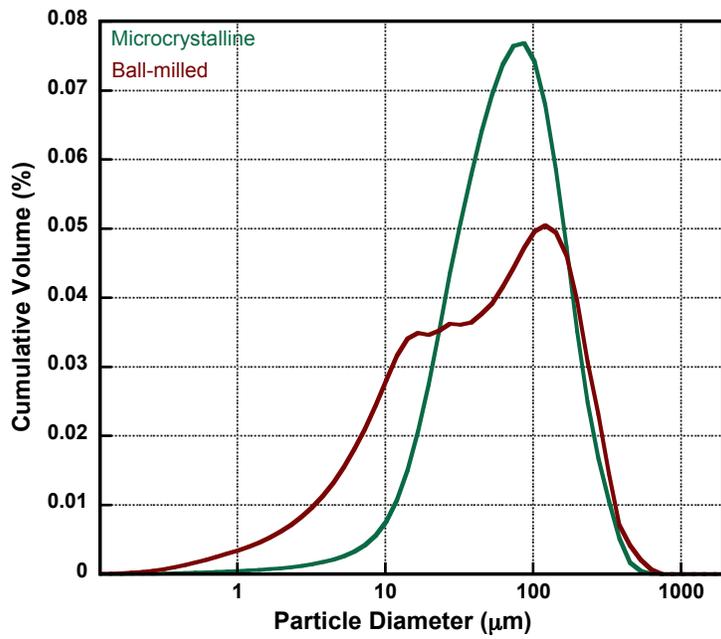

Figure 4-4. Particle size distribution for microcrystalline (green) and ball-milled cellulose (red).

The increment in amorphous content as well as the increase in surface area caused by the reduction in particle size causes an increase in cellulose conversion and hexitols yield as seen in Figure 4-5, Figure 4-6 and Table 4-2. These results are consistent with the behavior observed in previous reports.[70,172] The hydrolysis of cellulose occurs first in the amorphous regions and more rapidly if ball-milled cellulose is used, than for the crystalline material, as seen for all reactions presented in Figure 4-5. Without catalyst (entries 2 and 4) ball-milled cellulose exhibits a higher conversion and yield towards sugars than microcrystalline cellulose. For ruthenium supported on amorphous niobium phosphate (Ru/NbOPO$_4$ B2), the conversion increases from 58% for microcrystalline cellulose (Entry 2) to 96% for ball-milled cellulose (Entry 5). The cellulose treatment also causes a small increase in the yields towards hexitols, hydrogenolysis products and furfurals, when a cellulose to catalyst ratio of 10 is used during reaction. When the crystalline niobium phosphate (Ru/NbOPO$_4$ B1) is used as support the increase in conversion is similar (from 61% to 96%) but there is a larger increase in the yield towards sugar alcohols from 19% (Entry 3) to 45% (Entry 6) and a slight decrease in the yield towards hydrogenolysis products, due to lower cellulose to catalyst ratio (c:c = 3.3).

Figure 4-5. Effect of cellulose crystallinity on cellulose conversion. The reaction conditions with no catalyst present were 1 g of cellulose, 483 K, 1 h, 50 mL water and 35 bar of H_2. Both niobium phosphate reactions were run at 503 K, 0.5 h, 50 mL of water and 35 bar of H_2. The cellulose to catalyst ratio was the only parameter different in both reactions, cellulose to catalyst ratio of 10 for Ru/NbOPO$_4$ B2 and cellulose to catalyst ratio of 3.3 for Ru/NBOPO$_4$ B1. Microcrystalline (Micro) and Ball-milled (BM).
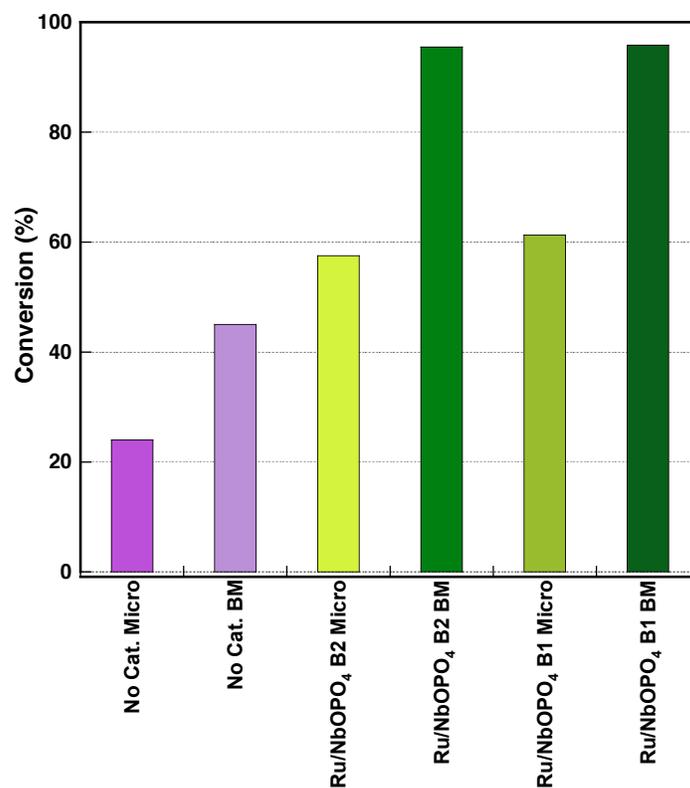
Figure 4-6. Effect of cellulose crystallinity on the yields. The reaction conditions with no catalyst present were 1 g of cellulose, 483 K, 1 h, 50 mL water and 35 bar of H₂. Both niobium phosphate reactions were run at 503 K, 0.5 h, 50 mL of water and 35 bar of H₂. The cellulose to catalyst ratio was the only parameter different in both reactions, cellulose to catalyst ratio of 10 for Ru/NbOPO₄ B2 and cellulose to catalyst ratio of 3.3 for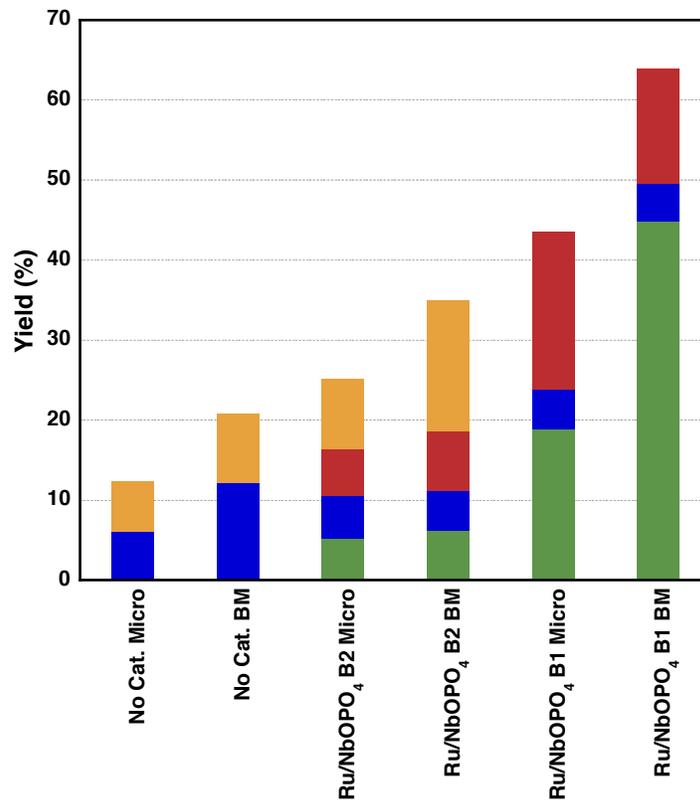 Ru/NBOPO₄ B1. Microcrystalline (Micro) and Ball-milled (BM) cellulose. Reaction products: sugar alcohols (green), sugars (blue), hydrogenolysis products (red) and furfurals (yellow).

Table 4-2. Reaction results for the effect of cellulose crystallinity.

Entry	Samples	Conversion (%)[a]	Yield (%)[b]			
			SA	S	H	F
	Microcrystalline					
1	No catalyst	24	0	6	0	6
2	Ru/NbOPO₄ B2	58	5	5	6	9
3	Ru/NbOPO₄ B1	61	19	5	20	0
	Ball-milled					
4	No catalyst	45	0	12	0	9
5	Ru/NbOPO₄ B2	96	6	5	8	16
6	Ru/NbOPO₄ B1	96	45	5	14	0

[a]The reaction conditions with no catalyst present were 1 g of cellulose, 483 K, 1 h, 50 mL water and 35 bar of H_2. Both niobium phosphate reactions were run at 503 K, 0.5 h, 50 mL of water and 35 bar of H_2. The cellulose to catalyst ratio was the only parameter different in both reactions, cellulose to catalyst ratio of 10 for Ru/NbOPO₄ B2 and cellulose to catalyst ratio of 3.3 for Ru/NBOPO₄ B1.
[b]SA= sugar alcohols, S= sugars, H= hydrogenolysis, F= furfurals.

The effect of cellulose to catalyst ratio was also investigated using the niobium phosphate catalysts, as shown in Table 4-3. A decrease in the cellulose to catalyst ratio results in higher hexitols yields. The yields are calculated using the carbon molar amount in the product by the total carbon amount in the starting material.[81] In previous studies the cellulose to catalyst ratios were studied between 1 to 10. As seen in Table 4-3, both niobium phosphate supports exhibit an increase in the hexitols yields when the cellulose to catalyst ratio is decreased. For Ru/NbOPO₄ B2 no significant difference in conversion was appreciated when ball-milled cellulose was used for the two cellulose to catalyst ratios used, but there was an increase in sugar alcohols yields and no presence of furfurals was observed when the ratio was lower. The formation of these furfural products (5-hydroxymethyl furfural and furfural) for cellulose to catalyst ratio of 10 in Ru/NbOPO₄ B2 could be attributed to a catalyst not well reduced and the high amount of cellulose used for the reaction.

Table 4-3. Effect of cellulose to catalyst ratio on the catalytic performance for the conversion of ball-milled cellulose.

Samples	Cellulose: Catalyst	Conversion (%)[a]	Yield (%)[b]			
			SA	S	H	F
Ru/ NbOPO$_4$ B2	10.1	96	6	5	8	16
	3.3	93	34	4	22	0
Ru/ NbOPO$_4$ B1	9.9	85	42	3	15	0
	3.3	96	45	5	14	0

[a]Reaction conditions: 503 K, 0.5 h, 50 mL of water and 35 bar of H$_2$.
[b]SA= sugar alcohols, S= sugars, H= hydrogenolysis, F= furfurals.

4.2.1.3 *Effect of temperature and reaction time*

Reaction temperature and time also influence the catalytic performance of ball-milled cellulose, as seen in Figure 4-7 and Figure 4-8 for Ru/NbOPO$_4$ B1. The conditions studied were temperatures of 483 K and 503 K, and reaction times that go from 0.08 to 2 h. The activities for this type of catalyst were compared with reactions in the absence of a catalyst. As mentioned before, an increase in the hydronium ion concentration increases the cellulose conversion. A temperature of 503 K, the ionization constant of water is 600 times the ionization constant at ambient temperature.[133] When we compare the results without a catalyst at the two temperatures, as the reaction time is increased there is a non-linear increase in the conversion. That increase in conversion appears to pass through a maximum close to 1 h of reaction (65% increases to 90%). Addition of Ru/NbOPO$_4$ B1 to the reaction at 483 K causes an almost constant increase in conversion for all reaction times. When the reaction is conducted in the presence of Ru/NbOPO$_4$ B1 at 503 K, we observed a similar trend for the conversion as a function of reaction time for the reaction without catalyst, but the curve is displaced to significant lower times. For ball-milled cellulose 100% conversion was obtained for Ru/NbOPO$_4$ B1 at 503 K and 1 h of reaction, compared to the 2 h of reaction needed to obtain 98% of conversion when the reaction without catalyst is conducted. Figure 4-8 illustrates the yields for Ru/NbOPO$_4$ B1 as a function of

temperature and time. At a reaction temperature of 483K, a reduction of sugars yields and an increase in hexitol yields is observed. On the other hand, for a reaction temperature of 503 K, it was observed that the hexitols yields goes through a maximum with a 45% of performance at 0.5 h of reaction, which was sufficient time to hydrogenate most of the sugars. Additionally, an increase in hydrogenolysis products was obtained increasing the reaction time due to the transformation of sugar alcohols into glycerol, erythritol and ethylene glycol. Also, Ru/NbOPO$_4$ B1 achieved 76% of overall yields to hexitols, sugars and hydrogenolysis products at reaction conditions of 1 h and 503 K for a 100% of ball-milled cellulose conversion, which demonstrated the good catalytic performance of this material.
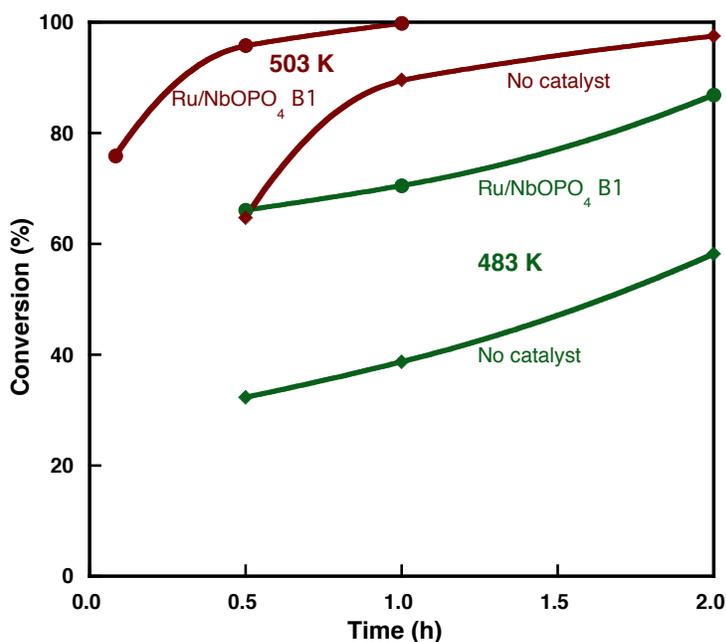

Figure 4-7. Cellulose conversion as a function of reaction time and temperature for Ru/NbOPO$_4$ B1 (circles) and the reaction in the absence of a catalyst (diamonds) with a cellulose to catalyst ratio of 3.3, 35 bar of H$_2$ and ball-milled cellulose. Temperatures of analysis were 483 K (green) and 503 K (red).
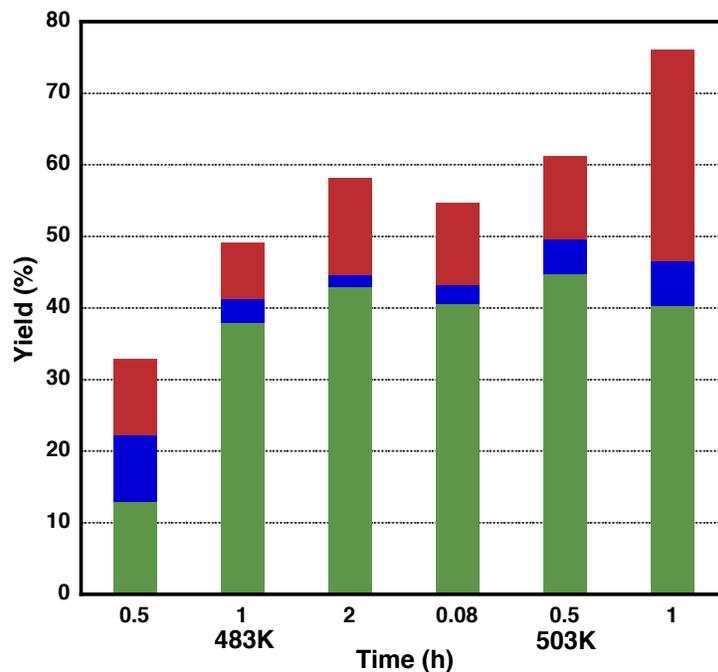
Figure 4-8. Yields as a function of reaction time and temperature for Ru/NbOPO₄ B1. Temperatures of analysis were 483 K and 503 K. Reaction times 0.08 h ≤ t ≤ 2 h. Reaction products: sugar alcohols (green), sugars (blue) and hydrogenolysis products (red).